

MULTIPHYSICS FINITE ELEMENT METHODS FOR A POROELASTICITY MODEL*

XIAOBING FENG[†], ZHIHAO GE[‡], AND YUKUN LI[§]

Abstract. This paper concerns with finite element approximations of a quasi-static poroelasticity model in displacement-pressure formulation which describes the dynamics of poro-elastic materials under an applied mechanical force on the boundary. To better describe the multiphysics process of deformation and diffusion for poro-elastic materials, we first present a reformulation of the original model by introducing two pseudo-pressures, one of them is shown to satisfy a diffusion equation, we then propose a time-stepping algorithm which decouples (or couples) the reformulated PDE problem at each time step into two sub-problems, one of which is a generalized Stokes problem for the displacement vector field (of the solid network of the poro-elastic material) along with one pseudo-pressure field and the other is a diffusion problem for the other pseudo-pressure field (of the solvent of the material). To make this multiphysics approach feasible numerically, two critical issues must be resolved: the first one is the uniqueness of the generalized Stokes problem and the other is to find a good boundary condition for the diffusion equation so that it also becomes uniquely solvable. To address the first issue, we discover certain conserved quantities for the PDE solution which provide ideal candidates for a needed boundary condition for the pseudo-pressure field. The solution to the second issue is to use the generalized Stokes problem to generate a boundary condition for the diffusion problem. A practical advantage of the time-stepping algorithm allows one to use any convergent Stokes solver (and its code) together with any convergent diffusion equation solver (and its code) to solve the poroelasticity model. In the paper, the Taylor-Hood mixed finite element method combined with the P_1 -conforming finite element method is used as an example to demonstrate the viability of the proposed multiphysics approach. It is proved that the solutions of the fully discrete finite element methods fulfill a discrete energy law which mimics the differential energy law satisfied by the PDE solution and converges optimally in the energy norm. Moreover, it is showed that the proposed formulation also has a built-in mechanism to overcome so-called “locking phenomenon” associated with the numerical approximations of the poroelasticity model. Numerical experiments are presented to show the performance of the proposed approach and methods and to demonstrate the absence of “locking phenomenon” in our numerical experiments. The paper also presents a detailed PDE analysis for the poroelasticity model, especially, it is proved that this model converges to the well-known Biot’s consolidation model from soil mechanics as the constrained specific storage coefficient tends to zero. As a result, the proposed approach and methods are robust under such a limit process.

Key words. Poroelasticity, deformation and diffusion, generalized Stokes equations, finite element methods, inf-sup condition, fully discrete schemes, error estimates.

AMS subject classifications. 65M12, 65M15, 65M60,

1. Introduction. A poroelastic material (or medium) is a fluid-solid interaction system at pore scale and poromechanics is a branch of continuum mechanics and acoustics that studies the behavior of fluid-saturated porous materials. If the solid is an elastic material, then the subject of the study is known as poroelasticity. Moreover, the elastic material may be governed by linear or nonlinear constitutive law, which then leads respectively to linear and nonlinear poroelasticity. Examples of

*LAST UPDATE: September 2, 2021

[†]Department of Mathematics, The University of Tennessee, Knoxville, TN 37996, U.S.A. (xfeng@math.utk.edu). The work of this author was partially supported by the NSF grants DMS-1016173 and DMS-1318486.

[‡]Institute of Applied Mathematics, School of Mathematics and Information Sciences, Henan University, Kaifeng, Henan Province 475004, P. R. China (zhihaoge@gmail.com). The work of this author was partially supported by the National Natural Science Foundation of China grant #10901047.

[§]Department of Mathematics, The University of Tennessee, Knoxville, TN 37996, U.S.A. (yli@math.utk.edu). The work of this author was partially supported by the NSF grants DMS-1016173 and DMS-1318486.

poroelastic materials include soil, polymer gels, and medicine pills, just name a few. Poroelastic materials exhibit an important state of matter found in a wide variety of mechanical, biomedical and chemical systems (cf. [7, 9, 23, 24, 26] and the references therein). They also possess some fascinating properties, in particular, they display thixotropy which means that they become fluid when agitated, but resolidify when resting. In general, the behavior of a poroelastic material is described by a multiphysics fluid-solid interaction process at pore scale. Unlike standard (macroscopic) fluid-solid interaction systems, some physical phenomena of the multiphysics process of the poroelastic material may not be explicitly revealed in its mathematical model, instead, they are hidden in the model. This is indeed the case for the poroelasticity model to be studied in this paper.

This paper considers a general quasi-static model of linear poroelasticity which is broad enough to contain the well-known Biot's consolidation model from soil mechanics (cf. [19, 21]) and the Doi's model for polymer gels (cf. [11, 26]). The quasi-static feature is due to the assumption that the acceleration of the solid (described by the second order time derivative of the displacement vector field) is assumed to be negligible. We refer the reader to [7, 17, 24] for a derivation of the model and to [22] for its mathematical analysis. When the parameter c_0 , called the constrained specific storage coefficient, vanishes in the model, it reduces into the above mentioned Boit's model and Doi's model arising from two distinct applications. Their mathematical analysis can be found in [11] and their finite element numerical approximations based on two very different approaches were carried out in [19, 11], respectively. In [17, 18] the authors proposed and analyzed a semi-discrete and a fully discrete mixed finite element method which simultaneously approximate the pressure and its gradient along with the displacement vector field. Since the implicit Euler scheme is used for the time discretization, a combined linear system must be solved at each time step. It is observed in the numerical tests that the proposed fully discrete mixed finite method may exhibit a "locking phenomenon" in the sense that the computed pressure oscillates and its accuracy deteriorate when a rapidly changed initial pressure is given, as explained in the [16] that such a "locking phenomenon" is caused by the difficulty of satisfying the nearly divergence-free condition of \mathbf{u} for very small time $t > 0$.

The goal of this paper is to present a multiphysics approach for approximating the poroelasticity model. A key idea of this approach is to derive a multiphysics reformulation for the original model which clearly reveals the underlying multiple physics process (i.e., the deformation and diffusion) of the pore-scale fluid-solid interaction system. To the end, two pseudo-pressures are introduced, one of them is shown to satisfy a diffusion equation, while the displacement vector field along with the other pseudo-pressure variable is shown to satisfy a generalized Stokes system. It should be noted that the original pressure is eliminated in the reformulation, thus, it is not approximated as a primary (unknown) variable, instead, it is computed as a linear combination of the two pseudo-pressures. Based on this multiphysics reformulation we then propose a time-stepping algorithm which decouples (or couples) the reformulated PDE problem at each time step into two sub-problems, a generalized Stokes problem for the displacement vector field along with a pseudo-pressures and a diffusion problem for another pseudo-pressure field. To make this multiphysics approach feasible numerically, two critical issue must be resolved: the first one is the uniqueness of the generalized Stokes problem and the other is to find a good boundary condition for the diffusion equation so that it also becomes uniquely solvable. To overcome these difficulties, we discover certain conserved quantities for the PDE solution which

can be imposed as needed boundary conditions for the subproblems. Moreover, we demonstrate that, regardless the choice of discretization methods, the proposed formulation has a built-in mechanism to overcome the “locking phenomenon” associated with numerical approximations of the poroelasticity model.

The remainder of this paper is organized as follows. In Section 2 we present a complete PDE analysis of the poroelasticity model which emphasizes the energy law of the underlying model. Several conserved quantities are derived for the PDE solution. Moreover, it is proved that the poroelasticity model converges to the Biot’s consolidation model as the constrained specific storage coefficient $c_0 \rightarrow 0$. In Section 3 we propose and analyze some fully discrete finite element methods based on the above mentioned multiphysics reformulation. Both coupled and decoupled time-stepping are considered and compared. The Taylor-Hood mixed finite element method combined with the P_1 -conforming finite element method is chosen as an example for spatial discretization. It is proved that the solutions of the fully discrete finite element methods fulfill a discrete energy law which mimics the differential energy law satisfied by the PDE solution. Optimal order error estimates in the energy norm are also established. Finally, in Section 4, several benchmark numerical experiments are provided to show the performance of the proposed approach and methods, and to demonstrate the absence of “locking phenomenon” in our numerical experiments.

2. PDE model and its analysis.

2.1. Preliminaries. $\Omega \subset \mathbb{R}^d$ ($d = 1, 2, 3$) denotes a bounded polygonal domain with the boundary $\partial\Omega$. The standard function space notation is adopted in this paper, their precise definitions can be found in [4, 6, 25]. In particular, (\cdot, \cdot) and $\langle \cdot, \cdot \rangle$ denote respectively the standard $L^2(\Omega)$ and $L^2(\partial\Omega)$ inner products. For any Banach space B , we let $\mathbf{B} = [B]^d$, and use \mathbf{B}' to denote its dual space. In particular, we use $(\cdot, \cdot)_{\text{dual}}$ and $\langle \cdot, \cdot \rangle_{\text{dual}}$ to denote the dual product on $(\mathbf{H}^1(\Omega))' \times \mathbf{H}^1(\Omega)$, and $\|\cdot\|_{L^p(B)}$ is a shorthand notation for $\|\cdot\|_{L^p((0,T);B)}$.

We also introduce the function spaces

$$L_0^2(\Omega) := \{q \in L^2(\Omega); (q, 1) = 0\}, \quad \mathbf{X} := \mathbf{H}^1(\Omega).$$

It is well known [25] that the following so-called inf-sup condition holds in the space $\mathbf{X} \times L_0^2(\Omega)$:

$$(2.1) \quad \sup_{\mathbf{v} \in \mathbf{X}} \frac{(\operatorname{div} \mathbf{v}, \varphi)}{\|\nabla \mathbf{v}\|_{L^2(\Omega)}} \geq \alpha_0 \|\varphi\|_{L^2(\Omega)} \quad \forall \varphi \in L_0^2(\Omega), \quad \alpha_0 > 0.$$

Let

$$\mathbf{RM} := \{\mathbf{r} := \mathbf{a} + \mathbf{b} \times x; \mathbf{a}, \mathbf{b}, x \in \mathbb{R}^d\}$$

denote the space of infinitesimal rigid motions. It is well known [3, 13, 25] that \mathbf{RM} is the kernel of the strain operator ε , that is, $\mathbf{r} \in \mathbf{RM}$ if and only if $\varepsilon(\mathbf{r}) = 0$. Hence, we have

$$(2.2) \quad \varepsilon(\mathbf{r}) = 0, \quad \operatorname{div} \mathbf{r} = 0 \quad \forall \mathbf{r} \in \mathbf{RM}.$$

Let $\mathbf{L}_\perp^2(\partial\Omega)$ and $\mathbf{H}_\perp^1(\Omega)$ denote respectively the subspaces of $\mathbf{L}^2(\partial\Omega)$ and $\mathbf{H}^1(\Omega)$ which are orthogonal to \mathbf{RM} , that is,

$$\begin{aligned} \mathbf{H}_\perp^1(\Omega) &:= \{\mathbf{v} \in \mathbf{H}^1(\Omega); (\mathbf{v}, \mathbf{r}) = 0 \forall \mathbf{r} \in \mathbf{RM}\}, \\ \mathbf{L}_\perp^2(\partial\Omega) &:= \{\mathbf{g} \in \mathbf{L}^2(\partial\Omega); \langle \mathbf{g}, \mathbf{r} \rangle = 0 \forall \mathbf{r} \in \mathbf{RM}\}. \end{aligned}$$

It is well known [10] that there exists a constant $c_1 > 0$ such that

$$\inf_{\mathbf{r} \in \mathbf{RM}} \|\mathbf{v} + \mathbf{r}\|_{L^2(\Omega)} \leq c_1 \|\varepsilon(\mathbf{v})\|_{L^2(\Omega)} \quad \forall \mathbf{v} \in \mathbf{H}^1(\Omega).$$

Hence, for each $\mathbf{v} \in \mathbf{H}_\perp^1(\Omega)$ there holds

$$(2.3) \quad \|\mathbf{v}\|_{L^2(\Omega)} = \inf_{\mathbf{r} \in \mathbf{RM}} \sqrt{\|\mathbf{v} + \mathbf{r}\|_{L^2(\Omega)}^2 - \|\mathbf{r}\|_{L^2(\Omega)}^2} \leq c_1 \|\varepsilon(\mathbf{v})\|_{L^2(\Omega)},$$

which and the well-known Korn's inequality [10] yield that for some $c_2 > 0$

$$(2.4) \quad \begin{aligned} \|\mathbf{v}\|_{H^1(\Omega)} &\leq c_2 [\|\mathbf{v}\|_{L^2(\Omega)} + \|\varepsilon(\mathbf{v})\|_{L^2(\Omega)}] \\ &\leq c_2(1 + c_1) \|\varepsilon(\mathbf{v})\|_{L^2(\Omega)} \quad \forall \mathbf{v} \in \mathbf{H}_\perp^1(\Omega). \end{aligned}$$

By Lemma 2.1 of [3] we know that for any $q \in L^2(\Omega)$, there exists $\mathbf{v} \in \mathbf{H}_\perp^1(\Omega)$ such that $\operatorname{div} \mathbf{v} = q$ and $\|\mathbf{v}\|_{H^1(\Omega)} \leq C\|q\|_{L^2(\Omega)}$. An immediate consequence of this lemma is that there holds the following alternative version of the inf-sup condition:

$$(2.5) \quad \sup_{\mathbf{v} \in \mathbf{H}_\perp^1(\Omega)} \frac{(\operatorname{div} \mathbf{v}, \varphi)}{\|\nabla \mathbf{v}\|_{L^2(\Omega)}} \geq \alpha_1 \|\varphi\|_{L^2(\Omega)} \quad \forall \varphi \in L_0^2(\Omega), \quad \alpha_1 > 0.$$

Throughout the paper, we assume $\Omega \subset \mathbb{R}^d$ is a bounded polygonal domain such that $\Delta : H_0^1(\Omega) \cap H^2(\Omega) \rightarrow L^2(\Omega)$ is an isomorphism (cf. [8, 13]). In addition, C is used to denote a generic positive (pure) constant which may be different in different places.

2.2. PDE model and its multiphysics reformulation. The quasi-static poroelasticity model to be studied in this paper is given by (cf. [17])

$$(2.6) \quad -\operatorname{div} \sigma(\mathbf{u}) + \alpha \nabla p = \mathbf{f} \quad \text{in } \Omega_T := \Omega \times (0, T) \subset \mathbb{R}^d \times (0, T),$$

$$(2.7) \quad (c_0 p + \alpha \operatorname{div} \mathbf{u})_t + \operatorname{div} \mathbf{v}_f = \phi \quad \text{in } \Omega_T,$$

where

$$(2.8) \quad \sigma(\mathbf{u}) := \mu \varepsilon(\mathbf{u}) + \lambda \operatorname{div} \mathbf{u} I, \quad \varepsilon(\mathbf{u}) := \frac{1}{2} (\nabla \mathbf{u} + \nabla \mathbf{u}^T),$$

$$(2.9) \quad \mathbf{v}_f := -\frac{K}{\mu_f} (\nabla p - \rho_f \mathbf{g}).$$

Where \mathbf{u} denotes the displacement vector of the solid and p denotes the pressure of the solvent. \mathbf{f} is the body force. I denotes the $d \times d$ identity matrix and $\varepsilon(\mathbf{u})$ is known as the strain tensor. The parameters in the model are Lamé constants λ and μ , the (symmetric) permeability tensor K , the solvent viscosity μ_f , Biot-Willis constant α , and the constrained specific storage coefficient c_0 . In addition, $\sigma(\mathbf{u})$ is called the (effective) stress tensor. $\hat{\sigma}(\mathbf{u}, p) := \sigma(\mathbf{u}) - \alpha p I$ is the total stress tensor. \mathbf{v}_f is the volumetric solvent flux and (2.9) is the well-known Darcy's law. We assume that $\rho_f \neq 0$, which is a realistic assumption.

To close the above system, suitable boundary and initial conditions must also be prescribed. The following set of boundary and initial conditions will be considered in this paper:

$$(2.10) \quad \hat{\sigma}(\mathbf{u}, p) \mathbf{n} = \sigma(\mathbf{u}) \mathbf{n} - \alpha p \mathbf{n} = \mathbf{f}_1 \quad \text{on } \partial \Omega_T := \partial \Omega \times (0, T),$$

$$(2.11) \quad \mathbf{v}_f \cdot \mathbf{n} = -\frac{K}{\mu_f} (\nabla p - \rho_f \mathbf{g}) \cdot \mathbf{n} = \phi_1 \quad \text{on } \partial \Omega_T,$$

$$(2.12) \quad \mathbf{u} = \mathbf{u}_0, \quad p = p_0 \quad \text{in } \Omega \times \{t = 0\}.$$

We note that in some engineering literature the second Lamé constant μ is also called the *shear modulus* and denoted by G , and $B := \lambda + \frac{2}{3}G$ is called the *bulk modulus*. λ, μ and B are computed from the *Young's modulus* E and the *Poisson ratio* ν by the following formulas:

$$\lambda = \frac{E\nu}{(1+\nu)(1-2\nu)}, \quad \mu = G = \frac{E}{2(1+\nu)}, \quad B = \frac{E}{3(1-2\nu)}.$$

Unlike the existing approaches in the literature [17, 19], in this paper we will not approximate the above original model directly, instead, we first derive a (multiphysics) reformulation for the model, we then approximate the reformulated model. This is a key idea of this paper and it will be seen in the later sections that this new approach is advantageous. To the end, we introduce new variables

$$q := \operatorname{div} \mathbf{u}, \quad \eta := c_0 p + \alpha q, \quad \xi := \alpha p - \lambda q.$$

It is easy to check that

$$(2.13) \quad p = \kappa_1 \xi + \kappa_2 \eta, \quad q = \kappa_1 \eta - \kappa_3 \xi,$$

where

$$(2.14) \quad \kappa_1 := \frac{\alpha}{\alpha^2 + \lambda c_0}, \quad \kappa_2 := \frac{\lambda}{\alpha^2 + \lambda c_0}, \quad \kappa_3 := \frac{c_0}{\alpha^2 + \lambda c_0}.$$

Then (2.6)–(2.9) can be written as

$$(2.15) \quad -\mu \operatorname{div} \varepsilon(\mathbf{u}) + \nabla \xi = \mathbf{f} \quad \text{in } \Omega_T,$$

$$(2.16) \quad \kappa_3 \xi + \operatorname{div} \mathbf{u} = \kappa_1 \eta \quad \text{in } \Omega_T,$$

$$(2.17) \quad \eta_t - \frac{1}{\mu_f} \operatorname{div} [K(\nabla(\kappa_1 \xi + \kappa_2 \eta) - \rho_f \mathbf{g})] = \phi \quad \text{in } \Omega_T,$$

where p and q are related to ξ and η through the algebraic equations in (2.13)

It is now clear that (\mathbf{u}, ξ) satisfies a generalized Stokes problem and η satisfies a diffusion problem. This new formulation reveals the underlying deformation and diffusion multiphysics process which occurs in the poroelastic material. In particular, the diffusion part of the process is hidden in the original formulation but is apparent in the new formulation. To make use the above reformulation for computation, we need to address a crucial issue of the uniqueness for the generalized Stokes problem and the diffusion problem after they are decoupled. The difficulty will be overcome by discovering some invariant quantities for the solution of the PDE model and using them to impose some appropriate boundary conditions for both subproblems (cf. Lemma 2.7).

2.3. Analysis of the PDE model. We start this section with a definition of weak solutions to problem (2.6)–(2.12). For convenience, we assume that $\mathbf{f}, \mathbf{f}_1, \phi$ and ϕ_1 all are independent of t in the remaining of the paper. We note that all the results of this paper can be easily extended to the time-dependent case.

DEFINITION 2.1. *Let $\mathbf{u}_0 \in \mathbf{H}^1(\Omega), \mathbf{f} \in \mathbf{L}^2(\Omega), \mathbf{f}_1 \in \mathbf{L}^2(\partial\Omega), p_0 \in L^2(\Omega), \phi \in L^2(\Omega)$, and $\phi_1 \in L^2(\partial\Omega)$. Assume $(\mathbf{f}, \mathbf{v}) + \langle \mathbf{f}_1, \mathbf{v} \rangle = 0$ for any $\mathbf{v} \in \mathbf{RM}$. Given $T > 0$, a tuple (\mathbf{u}, p) with*

$$\begin{aligned} \mathbf{u} &\in L^\infty(0, T; \mathbf{H}_\perp^1(\Omega)), & p &\in L^2(0, T; H^1(\Omega)), \\ (c_0 p + \alpha \operatorname{div} \mathbf{u})_t &\in L^2(0, T; H^{-1}(\Omega)), & c_0^{\frac{1}{2}} p &\in L^\infty(0, T; L^2(\Omega)), \end{aligned}$$

is called a weak solution to (2.6)–(2.12), if there hold for almost every $t \in [0, T]$

$$(2.18) \quad \begin{aligned} \mu(\varepsilon(\mathbf{u}), \varepsilon(\mathbf{v})) + \lambda(\operatorname{div} \mathbf{u}, \operatorname{div} \mathbf{v}) - \alpha(p, \operatorname{div} \mathbf{v}) \\ = (\mathbf{f}, \mathbf{v}) + \langle \mathbf{f}_1, \mathbf{v} \rangle \quad \forall \mathbf{v} \in \mathbf{H}^1(\Omega), \end{aligned}$$

$$(2.19) \quad \begin{aligned} ((c_0 p + \alpha \operatorname{div} \mathbf{u})_t, \varphi)_{\text{dual}} + \frac{1}{\mu_f} (K(\nabla p - \rho_f \mathbf{g}), \nabla \varphi) \\ = (\phi, \varphi) + \langle \phi_1, \varphi \rangle \quad \forall \varphi \in H^1(\Omega), \end{aligned}$$

$$(2.20) \quad \mathbf{u}(0) = \mathbf{u}_0, \quad p(0) = p_0.$$

Similarly, we can weak solutions to problem (2.15)–(2.17), (2.10)–(2.12).

DEFINITION 2.2. Let $\mathbf{u}_0 \in \mathbf{H}^1(\Omega)$, $\mathbf{f} \in \mathbf{L}^2(\Omega)$, $\mathbf{f}_1 \in \mathbf{L}^2(\partial\Omega)$, $p_0 \in L^2(\Omega)$, $\phi \in L^2(\Omega)$, and $\phi_1 \in L^2(\partial\Omega)$. Assume $(\mathbf{f}, \mathbf{v}) + \langle \mathbf{f}_1, \mathbf{v} \rangle = 0$ for any $\mathbf{v} \in \mathbf{RM}$. Given $T > 0$, a 5-tuple $(\mathbf{u}, \xi, \eta, p, q)$ with

$$\begin{aligned} \mathbf{u} &\in L^\infty(0, T; \mathbf{H}_\perp^1(\Omega)), & \xi &\in L^2(0, T; L^2(\Omega)), \\ \eta &\in L^\infty(0, T; L^2(\Omega)) \cap H^1(0, T; H^{-1}(\Omega)), & q &\in L^\infty(0, T; L^2(\Omega)), \\ p &\in L^2(0, T; H^1(\Omega)), \end{aligned}$$

is called a weak solution to (2.15)–(2.17), (2.10)–(2.12) if there hold for almost every $t \in [0, T]$

$$(2.21) \quad \mu(\varepsilon(\mathbf{u}), \varepsilon(\mathbf{v})) - (\xi, \operatorname{div} \mathbf{v}) = (\mathbf{f}, \mathbf{v}) + \langle \mathbf{f}_1, \mathbf{v} \rangle \quad \forall \mathbf{v} \in \mathbf{H}^1(\Omega),$$

$$(2.22) \quad \kappa_3(\xi, \varphi) + (\operatorname{div} \mathbf{u}, \varphi) = \kappa_1(\eta, \varphi) \quad \forall \varphi \in L^2(\Omega),$$

$$(2.23) \quad \begin{aligned} (\eta_t, \psi)_{\text{dual}} + \frac{1}{\mu_f} (K(\nabla(\kappa_1 \xi + \kappa_2 \eta) - \rho_f \mathbf{g}), \nabla \psi) \\ = (\phi, \psi) + \langle \phi_1, \psi \rangle \quad \forall \psi \in H^1(\Omega), \end{aligned}$$

$$(2.24) \quad p := \kappa_1 \xi + \kappa_2 \eta, \quad q := \kappa_1 \eta - \kappa_3 \xi,$$

$$(2.25) \quad \mathbf{u}(0) = \mathbf{u}_0, \quad p(0) = p_0,$$

$$(2.26) \quad q(0) = q_0 := \operatorname{div} \mathbf{u}_0, \quad \eta(0) = \eta_0 := c_0 p_0 + \alpha q_0.$$

REMARK 2.1. (a) After ξ and η are computed, p and q are simply updated by their algebraic expressions in (2.24).

(b) Equation (2.23) implicitly imposes the following boundary condition for η :

$$(2.27) \quad \kappa_2 K \frac{\partial \eta}{\partial n} = K \rho_f g \cdot n - \kappa_1 K \frac{\partial \xi}{\partial n}.$$

(c) It should be pointed out that the only reason for introducing the space $\mathbf{H}_\perp^1(\Omega)$ in the above two definitions is that the boundary condition (2.10) is a pure “Neumann condition”. If it is replaced by a pure Dirichlet condition or by a mixed Dirichlet-Neumann condition, there is no need to introduce this space. This fact will be used in our numerical experiments in Section 4. We also note that from the analysis point of view, the pure Neumann condition case is the most difficult case.

LEMMA 2.3. Every weak solution (\mathbf{u}, p) of problem (2.18)–(2.20) satisfies the following energy law:

$$(2.28) \quad E(t) + \frac{1}{\mu_f} \int_0^t (K(\nabla p - \rho_f \mathbf{g}), \nabla p) ds - \int_0^t (\phi, p) ds - \int_0^t \langle \phi_1, p \rangle ds = E(0)$$

for all $t \in [0, T]$, where

$$(2.29) \quad E(t) := \frac{1}{2} \left[\mu \|\varepsilon(\mathbf{u}(t))\|_{L^2(\Omega)}^2 + \lambda \|\operatorname{div} \mathbf{u}(t)\|_{L^2(\Omega)}^2 + c_0 \|p(t)\|_{L^2(\Omega)}^2 - 2\langle \mathbf{f}, \mathbf{u}(t) \rangle - 2\langle \mathbf{f}_1, \mathbf{u}(t) \rangle \right].$$

Moreover,

$$(2.30) \quad \|(c_0 p + \alpha \operatorname{div} \mathbf{u})_t\|_{L^2(0, T; H^{-1}(\Omega))} \leq \frac{K}{\mu_f} \|\nabla p - \rho_f \mathbf{g}\|_{L^2(\Omega_T)} + \|\phi\|_{L^2(\Omega_T)} + \|\phi_1\|_{L^2(\partial\Omega_T)} < \infty.$$

Proof. We only consider the case $\mathbf{u}_t \in \mathbf{L}^2((0, T); \mathbf{L}^2(\Omega))$, the general case can be converted into this case using the Steklov average technique (cf. [15, Chapter 2]). Setting $\varphi = p$ in (2.19) and $\mathbf{v} = \mathbf{u}_t$ in (2.18) yields for a.e. $t \in [0, T]$

$$(2.31) \quad ((c_0 p + \alpha \operatorname{div} \mathbf{u})_t, p(t))_{\text{dual}} + \frac{1}{\mu_f} (K(\nabla p - \rho_f \mathbf{g}), \nabla p) = (\phi, p) + \langle \phi_1, p \rangle,$$

$$(2.32) \quad \mu(\varepsilon(\mathbf{u}), \varepsilon(\mathbf{u}_t)) + \lambda(\operatorname{div} \mathbf{u}, \operatorname{div} \mathbf{u}_t) - \alpha(p, \operatorname{div} \mathbf{u}_t) = \langle \mathbf{f}, \mathbf{u}_t \rangle + \langle \mathbf{f}_1, \mathbf{u}_t \rangle.$$

Adding the above two equations and integrating the sum in t over the interval $(0, s)$ for any $s \in (0, T]$ yield

$$(2.33) \quad E(s) + \frac{1}{\mu_f} \int_0^s (K(\nabla p - \rho_f \mathbf{g}), \nabla p) dt - \int_0^s (\phi, p) dt - \int_0^s \langle \phi_1, p \rangle dt = E(0),$$

where $E(\cdot)$ is given by (2.29). Here we have used the fact that \mathbf{f} and \mathbf{f}_1 are independent of t . Hence, (2.28) holds.

(2.30) follows immediately from (2.28) and (2.19). The proof is complete. \square

Likewise, weak solutions of (2.21)–(2.26) satisfy a similar energy law which is a rewritten version of (2.28) in the new variables.

LEMMA 2.4. *Every weak solution $(\mathbf{u}, \xi, \eta, p, q)$ of problem (2.21)–(2.26) satisfies the following energy law:*

$$(2.34) \quad J(t) + \frac{1}{\mu_f} \int_0^t (K(\nabla p - \rho_f \mathbf{g}), \nabla p) ds - \int_0^t (\phi, p) ds - \int_0^t \langle \phi_1, p \rangle ds = J(0)$$

for all $t \in [0, T]$, where

$$(2.35) \quad J(t) := \frac{1}{2} \left[\mu \|\varepsilon(\mathbf{u}(t))\|_{L^2(\Omega)}^2 + \kappa_2 \|\eta(t)\|_{L^2(\Omega)}^2 + \kappa_3 \|\xi(t)\|_{L^2(\Omega)}^2 - 2\langle \mathbf{f}, \mathbf{u}(t) \rangle - 2\langle \mathbf{f}_1, \mathbf{u}(t) \rangle \right].$$

Moreover,

$$(2.36) \quad \|\eta_t\|_{L^2(0, T; H^{-1}(\Omega))} \leq \frac{K}{\mu_f} \|\nabla p - \rho_f \mathbf{g}\|_{L^2(\Omega_T)} + \|\phi\|_{L^2(\Omega_T)} + \|\phi_1\|_{L^2(\partial\Omega_T)} < \infty.$$

Proof. Again, we only consider the case that $\mathbf{u}_t \in L^2(0, T; L^2(\Omega))$. Setting $\mathbf{v} = \mathbf{u}_t$ in (2.21), differentiating (2.22) with respect to t followed by taking $\varphi = \xi$, and setting

$\psi = p = \kappa_1 \xi + \kappa_2 \eta$ in (2.23); adding the resulting equations and integrating in t yield the desired equality (2.34). The inequality (2.36) follows immediately from (2.23) and (2.34). \square

The above energy law immediately implies the following solution estimates.

LEMMA 2.5. *There exists a positive constant $C_1 = C_1(\|\mathbf{u}_0\|_{H^1(\Omega)}, \|p_0\|_{L^2(\Omega)}, \|\mathbf{f}\|_{L^2(\Omega)}, \|\mathbf{f}_1\|_{L^2(\partial\Omega)}, \|\phi\|_{L^2(\Omega)}, \|\phi_1\|_{L^2(\partial\Omega)})$ such that*

$$(2.37) \quad \begin{aligned} & \sqrt{\mu} \|\varepsilon(\mathbf{u})\|_{L^\infty(0,T;L^2(\Omega))} + \sqrt{\kappa_2} \|\eta\|_{L^\infty(0,T;L^2(\Omega))} \\ & + \sqrt{\kappa_3} \|\xi\|_{L^\infty(0,T;L^2(\Omega))} + \sqrt{\frac{K}{\mu_f}} \|\nabla p\|_{L^2(0,T;L^2(\Omega))} \leq C_1. \end{aligned}$$

$$(2.38) \quad \|\mathbf{u}\|_{L^\infty(0,T;L^2(\Omega))} \leq C_1, \quad \|p\|_{L^\infty(0,T;L^2(\Omega))} \leq C_1 \left(1 + \sqrt{\frac{\kappa_3}{\kappa_1}}\right).$$

We note that (2.38) follows from (2.37), (2.3) and the relation $p = \kappa_1 \xi + \kappa_2 \eta$.

Furthermore, by exploiting the linearity of the PDE system, we have the following a priori estimates for the weak solution.

THEOREM 2.6. *Suppose that \mathbf{u}_0 and p_0 are sufficiently smooth, then there exists a positive constant $C_2 = C_2(C_1, \|\nabla p_0\|_{L^2(\Omega)})$ and $C_3 = C_3(C_1, C_2, \|\mathbf{u}_0\|_{H^2(\Omega)}, \|p_0\|_{H^2(\Omega)})$ such that there hold the following estimates for the solution to problem (2.15)–(2.17), (2.10)–(2.12):*

$$(2.39) \quad \begin{aligned} & \sqrt{\mu} \|\varepsilon(\mathbf{u}_t)\|_{L^2(0,T;L^2(\Omega))} + \sqrt{\kappa_2} \|\eta_t\|_{L^2(0,T;L^2(\Omega))} \\ & + \sqrt{\kappa_3} \|\xi_t\|_{L^2(0,T;L^2(\Omega))} + \sqrt{\frac{K}{\mu_f}} \|\nabla p\|_{L^\infty(0,T;L^2(\Omega))} \leq C_2. \end{aligned}$$

$$(2.40) \quad \begin{aligned} & \sqrt{\mu} \|\varepsilon(\mathbf{u}_t)\|_{L^\infty(0,T;L^2(\Omega))} + \sqrt{\kappa_2} \|\eta_t\|_{L^\infty(0,T;L^2(\Omega))} \\ & + \sqrt{\kappa_3} \|\xi_t\|_{L^\infty(0,T;L^2(\Omega))} + \sqrt{\frac{K}{\mu_f}} \|\nabla p_t\|_{L^2(0,T;L^2(\Omega))} \leq C_3. \end{aligned}$$

$$(2.41) \quad \|\eta_{tt}\|_{L^2(H^{-1}(\Omega))} \leq \sqrt{\frac{K}{\mu_f}} C_3.$$

Proof. On noting that $\mathbf{f}, \mathbf{f}_1, \phi$ and ϕ_1 all are assumed to be independent of t , differentiating (2.21) and (2.22) with respect to t , taking $\mathbf{v} = \mathbf{u}_t$ and $\varphi = \xi_t$ in (2.21) and (2.22) respectively, and adding the resulting equations yield

$$(2.42) \quad \mu \|\varepsilon(\mathbf{u}_t)\|_{L^2(\Omega)}^2 = (q_t, \xi_t) = \kappa_1 (\eta_t, \xi_t) - \kappa_3 \|\xi_t\|_{L^2(\Omega)}^2.$$

Setting $\psi = p_t = \kappa_1 \xi_t + \kappa_2 \eta_t$ in (2.23) gives

$$(2.43) \quad \kappa_1 (\eta_t, \xi_t) + \kappa_2 \|\eta_t\|_{L^2(\Omega)}^2 + \frac{K}{2\mu_f} \frac{d}{dt} \|\nabla p - \rho_f \mathbf{g}\|_{L^2(\Omega)}^2 = \frac{d}{dt} [(\phi, p) + \langle \phi_1, p \rangle].$$

Adding (2.42) and (2.43) and integrating in t we get for $t \in [0, T]$

$$\begin{aligned} & \frac{K}{2\mu_f} \|\nabla p(t) - \rho_f \mathbf{g}\|_{L^2(\Omega)}^2 + \int_0^t \left[\mu \|\varepsilon(\mathbf{u}_t)\|_{L^2(\Omega)}^2 + \kappa_2 \|\eta_t\|_{L^2(\Omega)}^2 + \kappa_3 \|\xi_t\|_{L^2(\Omega)}^2 \right] ds \\ & = \frac{K}{2\mu_f} \|\nabla p_0 - \rho_f \mathbf{g}\|_{L^2(\Omega)}^2 + (\phi, p(t) - p_0) + \langle \phi_1, p(t) - p_0 \rangle, \end{aligned}$$

which readily infers (2.39).

To show (2.40), first differentiating (2.21) one time with respect to t and setting $\mathbf{v} = \mathbf{u}_{tt}$, differentiating (2.22) twice with respect to t and setting $\varphi = \xi_t$, and adding the resulting equations we get

$$(2.44) \quad \frac{\mu}{2} \frac{d}{dt} \|\varepsilon(\mathbf{u}_t)\|_{L^2(\Omega)}^2 = (q_{tt}, \xi_t) = \kappa_1 (\eta_{tt}, \xi_t) - \frac{\kappa_3}{2} \frac{d}{dt} \|\xi_t\|_{L^2(\Omega)}^2.$$

Second, differentiating (2.23) with respect t one time and taking $\psi = p_t = \kappa_1 \xi_t + \kappa_2 \eta_t$ yield

$$(2.45) \quad \kappa_1 (\eta_{tt}, \xi_t) + \frac{\kappa_2}{2} \frac{d}{dt} \|\eta_t\|_{L^2(\Omega)}^2 + \frac{K}{\mu_f} \|\nabla p_t\|_{L^2(\Omega)}^2 = 0.$$

Finally, adding the above two inequalities and integrating in t give for $t \in [0, T]$

$$(2.46) \quad \mu \|\varepsilon(\mathbf{u}_t(t))\|_{L^2(\Omega)}^2 + \kappa_2 \|\eta_t(t)\|_{L^2(\Omega)}^2 + \kappa_3 \|\xi_t(t)\|_{L^2(\Omega)}^2 + \frac{2K}{\mu_f} \int_0^t \|\nabla p_t\|_{L^2(\Omega)}^2 ds \\ = \mu \|\varepsilon(\mathbf{u}_t(0))\|_{L^2(\Omega)}^2 + \kappa_2 \|\eta_t(0)\|_{L^2(\Omega)}^2 + \kappa_3 \|\xi_t(0)\|_{L^2(\Omega)}^2.$$

Hence, (2.40) holds. (2.41) follows immediately from the following inequality

$$(\eta_{tt}, \psi) = -\frac{1}{\mu_f} (K \nabla p, \nabla \psi) \leq \frac{K}{\mu_f} \|\nabla p\|_{L^2(\Omega)} \|\nabla \psi\|_{L^2(\Omega)} \quad \forall \psi \in H_0^1(\Omega),$$

(2.40) and the definition of the H^{-1} -norm. The proof is complete. \square

REMARK 2.2. *As expected, the above high order norm solution estimates require $p_0 \in H^1(\Omega)$, $\mathbf{u}_t(0) \in \mathbf{L}^2(\Omega)$, $\eta_t(0) \in L^2(\Omega)$ and $\xi_t(0) \in L^2(\Omega)$. The values of $\mathbf{u}_t(0)$, $\eta_t(0)$ and $\xi_t(0)$ can be computed using the PDEs as follows. It follows from (2.17) that $\eta_t(0)$ satisfies*

$$\eta_t(0) = \phi + \frac{1}{\mu_f} \operatorname{div} [K(\nabla p_0 - \rho_f \mathbf{g})].$$

Hence $\eta_t(0) \in L^2(\Omega)$ provided that $p_0 \in H^2(\Omega)$.

To find $\mathbf{u}_t(0)$ and $\xi_t(0)$, differentiating (2.15) and (2.16) with respect to t and setting $t = 0$ we get

$$\begin{aligned} -\mu \operatorname{div} \varepsilon(\mathbf{u}_t(0)) + \nabla \xi_t(0) &= 0 && \text{in } \Omega, \\ \kappa_3 \xi_t(0) + \operatorname{div} \mathbf{u}_t(0) &= \kappa_1 \eta_t(0) && \text{in } \Omega. \end{aligned}$$

Hence, $\mathbf{u}_t(0)$ and $\xi_t(0)$ can be determined by solving the above generalized Stokes problem.

The next lemma shows that weak solutions of problem (2.21)–(2.26) preserve some “invariant” quantities, it turns out that these “invariant” quantities play a vital role in the construction of our time-splitting scheme to be introduced in the next section.

LEMMA 2.7. *Every weak solution $(\mathbf{u}, \xi, \eta, p, q)$ to problem (2.21)–(2.26) satisfies the following relations:*

$$(2.47) \quad C_\eta(t) := (\eta(\cdot, t), 1) = (\eta_0, 1) + [(\phi, 1) + \langle \phi_1, 1 \rangle] t, \quad t \geq 0.$$

$$(2.48) \quad C_\xi(t) := (\xi(\cdot, t), 1) = \frac{1}{d + \mu \kappa_3} [\mu \kappa_1 C_\eta(t) - (\mathbf{f}, x) - \langle \mathbf{f}_1, x \rangle].$$

$$(2.49) \quad C_q(t) := (q(\cdot, t), 1) = \kappa_1 C_\eta(t) - \kappa_3 C_\xi(t).$$

$$(2.50) \quad C_p(t) := (p(\cdot, t), 1) = \kappa_1 C_\xi(t) + \kappa_2 C_\eta(t).$$

$$(2.51) \quad C_{\mathbf{u}}(t) := \langle \mathbf{u}(\cdot, t) \cdot \mathbf{n}, 1 \rangle = C_q(t).$$

Proof. We first notice that equation (2.47) follows immediately from taking $\varphi \equiv 1$ in (2.23), which is a valid test function.

To prove (2.48), taking $\mathbf{v} = x$ in (2.21) and $\varphi = 1$ in (2.22), which are valid test functions, and using the identities $\nabla x = I$, $\operatorname{div} x = d$, and $\varepsilon(x) = I$, we get

$$(2.52) \quad \mu(\operatorname{div} \mathbf{u}, 1) - d(\xi, 1) = \langle \mathbf{f}, x \rangle + \langle \mathbf{f}_1, x \rangle,$$

$$(2.53) \quad (\operatorname{div} \mathbf{u}, 1) = \kappa_1(\eta, 1) - \kappa_3(\xi, 1).$$

Substituting (2.53) into (2.52) and using (2.47) yield

$$(2.54) \quad C_\xi(t) := (\xi(\cdot, t), 1) = \frac{1}{d + \mu\kappa_3} [\mu\kappa_1 C_\eta(t) - \langle \mathbf{f}, x \rangle - \langle \mathbf{f}_1, x \rangle].$$

Hence (2.48) holds. (2.49) follows immediately from (2.53), (2.47) and (2.48).

Finally, since $p = \kappa_1\xi + \kappa_2\eta$, (2.50) then follows from (2.47) and (2.48). (2.51) is an immediate consequence of $q = \operatorname{div} \mathbf{u}$ and the divergence theorem. The proof is complete. \square

REMARK 2.3. We note that C_η, C_ξ, C_q and C_p all are (known) linear functions of t , and they become (known) constants when $\phi \equiv 0$ and $\phi_1 \equiv 0$.

With the help of the above lemmas, we can show the solvability of problem (2.6)–(2.12).

THEOREM 2.8. Let $\mathbf{u}_0 \in \mathbf{H}^1(\Omega)$, $\mathbf{f} \in \mathbf{L}^2(\Omega)$, $\mathbf{f}_1 \in \mathbf{L}^2(\partial\Omega)$, $p_0 \in L^2(\Omega)$, $\phi \in L^2(\Omega)$, and $\phi_1 \in L^2(\partial\Omega)$. Suppose $\langle \mathbf{f}, \mathbf{v} \rangle + \langle \mathbf{f}_1, \mathbf{v} \rangle = 0$ for any $\mathbf{v} \in \mathbf{RM}$. Then there exists a unique solution to problem (2.6)–(2.12) in the sense of Definition 2.1, likewise, there exists a unique solution to problem (2.15)–(2.17), (2.10)–(2.12) in the sense of Definition 2.2.

Proof. We only outline the main steps of the proof and leave the details to the interested reader.

First, since the PDE system is linear, the existence of weak solution can be proved by the standard Galerkin method and compactness argument (cf. [25]). We note that the energy laws established in Lemmas 2.3 and 2.4 guarantee the required uniform estimates for the Galerkin approximate solutions.

Second, to show the uniqueness, suppose there are two sets of weak solutions, again by the linearity of the PDE system it is trivial to show that the difference of the solutions satisfy the same PDE system with *zero* initial and boundary data. The energy law immediately implies that the difference must be zero, hence, the uniqueness is verified. \square

We conclude this section by establishing a convergence result for the solution of problem (2.15)–(2.17), (2.10)–(2.12) when the constrained specific storage coefficient c_0 tends to 0. Such a convergence result is useful and significant for the following two reasons. First, as mentioned earlier, the poroelasticity model studied in this paper reduces into the well-known Biot's consolidation model from soil mechanics (cf. [19, 17]) and Doi's model for polymer gels (cf. [26, 11]). Second, it proves that the proposed approach and methods of this paper are robust under such a limit process.

THEOREM 2.9. Let $\mathbf{u}_0 \in \mathbf{H}^1(\Omega)$, $\mathbf{f} \in \mathbf{L}^2(\Omega)$, $\mathbf{f}_1 \in \mathbf{L}^2(\partial\Omega)$, $p_0 \in L^2(\Omega)$, $\phi \in L^2(\Omega)$, and $\phi_1 \in L^2(\partial\Omega)$. Suppose $\langle \mathbf{f}, \mathbf{v} \rangle + \langle \mathbf{f}_1, \mathbf{v} \rangle = 0$ for any $\mathbf{v} \in \mathbf{RM}$. Let $(\mathbf{u}_{c_0}, \eta_{c_0}, \xi_{c_0}, p_{c_0}, q_{c_0})$ denote the unique weak solution to problem (2.15)–(2.17), (2.10)–(2.12). Then there exists $(\mathbf{u}_*, \eta_*, \xi_*, p_*, q_*) \in \mathbf{L}^\infty(0, T; \mathbf{H}_\perp^1(\Omega)) \times L^\infty(0, T; L^2(\Omega)) \times L^\infty(0, T; L^2(\Omega)) \times L^\infty(0, T; L^2(\Omega)) \cap L^2(0, T; H^1(\Omega) \times L^\infty(0, T; L^2(\Omega))$ such that

$(\mathbf{u}_{c_0}, \eta_{c_0}, \xi_{c_0}, p_{c_0}, q_{c_0})$ converges weakly to $(\mathbf{u}_*, \eta_*, \xi_*, p_*, q_*)$ in the above product space as $c_0 \rightarrow 0$.

Proof. It follows immediately from (2.36)–(2.38) and Korn's inequality that

- \mathbf{u}_{c_0} is uniformly bounded (in c_0) in $\mathbf{L}^\infty(0, T; \mathbf{H}_\perp^1(\Omega))$.
- $\sqrt{\kappa_2} \eta_{c_0}$ is uniformly bounded (in c_0) in $L^\infty(0, T; L^2(\Omega)) \cap L^2(0, T; H^{-1}(\Omega))$.
- $\sqrt{\kappa_3} \xi_{c_0}$ is uniformly bounded (in c_0) in $L^\infty(0, T; L^2(\Omega))$.
- p_{c_0} is uniformly bounded (in c_0) in $L^\infty(0, T; L^2(\Omega)) \cap L^2(0, T; H^1(\Omega))$.
- q_{c_0} is uniformly bounded (in c_0) in $L^\infty(0, T; L^2(\Omega))$.

On noting that $\lim_{c_0 \rightarrow 0} \kappa_1 = \frac{1}{\alpha}$, $\lim_{c_0 \rightarrow 0} \kappa_2 = \frac{\lambda}{\alpha^2}$ and $\lim_{c_0 \rightarrow 0} \kappa_3 = 0$, by the weak compactness of reflexive Banach spaces and Aubin-Lions Lemma [10] we have that there exist $(\mathbf{u}_*, \eta_*, \xi_*, p_*, q_*) \in \mathbf{L}^\infty(0, T; \mathbf{H}_\perp^1(\Omega)) \times L^\infty(0, T; L^2(\Omega)) \times L^\infty(0, T; L^2(\Omega)) \times L^\infty(0, T; L^2(\Omega)) \cap L^2(0, T; H^1(\Omega)) \times L^\infty(0, T; L^2(\Omega))$ and a subsequence of $(\mathbf{u}_{c_0}, \eta_{c_0}, \xi_{c_0}, p_{c_0}, q_{c_0})$ (still denoted by the same notation) such that as $c_0 \rightarrow 0$ (a subsequence of c_0 , to be exact)

- \mathbf{u}_{c_0} converges to \mathbf{u}_* weak * in $\mathbf{L}^\infty(0, T; \mathbf{H}_\perp^1(\Omega))$ and weakly in $\mathbf{L}^2(0, T; \mathbf{H}_\perp^1(\Omega))$.
- $\sqrt{\kappa_2} \eta_{c_0}$ converges to $\frac{\sqrt{\lambda}}{\alpha} \eta_*$ weak * in $L^\infty(0, T; L^2(\Omega))$ and strongly in $L^2(\Omega_T)$.
- $\kappa_3 \xi_{c_0}$ converges to 0 strongly in $L^2(\Omega_T)$.
- p_{c_0} converges to p_* weak * in $L^\infty(0, T; L^2(\Omega))$ and weakly in $L^2(0, T; H^1(\Omega))$.
- q_{c_0} converges to p_* weak * in $L^\infty(0, T; L^2(\Omega))$ and weakly in $L^2(\Omega_T)$.

Then setting $c_0 \rightarrow 0$ in (2.21)–(2.26) yields (note that the dependence of the solution on c_0 is suppressed there)

$$\begin{aligned} \mu(\varepsilon(\mathbf{u}_*), \varepsilon(\mathbf{v})) - (\xi_*, \operatorname{div} \mathbf{v}) &= (\mathbf{f}, \mathbf{v}) + \langle \mathbf{f}_1, \mathbf{v} \rangle & \forall \mathbf{v} \in \mathbf{H}^1(\Omega), \\ (\operatorname{div} \mathbf{u}_*, \varphi) &= \frac{1}{\alpha} (\eta_*, \varphi) & \forall \varphi \in L^2(\Omega), \\ ((\eta_*)_t, \psi)_{\text{dual}} + \frac{1}{\mu_f} (K(\nabla(\alpha^{-1} + \lambda\alpha^{-2}\eta_*) - \rho_f \mathbf{g}), \nabla \psi) & \\ &= (\phi, \psi) + \langle \phi_1, \psi \rangle & \forall \psi \in H^1(\Omega), \\ p_* &:= \frac{1}{\alpha} \xi_* + \frac{\lambda}{\alpha^2} \eta_*, \quad q_* := \frac{1}{\alpha} \eta_*, \\ \mathbf{u}_*(0) &= \mathbf{u}_0, \\ q_*(0) = q_0 &:= \operatorname{div} \mathbf{u}_0, \quad \eta_*(0) = \eta_0 := \alpha q_0. \end{aligned}$$

Equivalently,

$$\begin{aligned} \mu(\varepsilon(\mathbf{u}_*), \varepsilon(\mathbf{v})) - (\xi_*, \operatorname{div} \mathbf{v}) &= (\mathbf{f}, \mathbf{v}) + \langle \mathbf{f}_1, \mathbf{v} \rangle & \forall \mathbf{v} \in \mathbf{H}^1(\Omega), \\ (\operatorname{div} \mathbf{u}_*, \varphi) &= (q_*, \varphi) & \forall \varphi \in L^2(\Omega), \\ \alpha((q_*)_t, \psi)_{\text{dual}} + \frac{1}{\mu_f} (K(\nabla p_* - \rho_f \mathbf{g}), \nabla \psi) &= (\phi, \psi) + \langle \phi_1, \psi \rangle & \forall \psi \in H^1(\Omega), \\ p_* &:= \frac{1}{\alpha} (\xi_* + \lambda q_*) \quad \text{or} \quad \xi_* = \alpha p_* - \lambda q_*, \\ \mathbf{u}_*(0) &= \mathbf{u}_0, \\ q_*(0) &= q_0 := \operatorname{div} \mathbf{u}_0. \end{aligned}$$

Hence, $(\mathbf{u}_*, \eta_*, \xi_*, p_*, q_*)$ is a weak solution of Biot's consolidation model (cf. [26, 11]). By the uniqueness of its solutions, we conclude that the whole sequence $(\mathbf{u}_{c_0}, \eta_{c_0}, \xi_{c_0}, p_{c_0}, q_{c_0})$ converges to $(\mathbf{u}_*, \eta_*, \xi_*, p_*, q_*)$ as $c_0 \rightarrow 0$ in the above sense. The proof is complete. \square

3. Fully discrete finite element methods. The goal of this section is to design and analyze some fully discrete finite element methods for the poroelasticity model based on the above new formulation. As the time stepping is vital for the overall methods, we first introduce our time-stepping schemes at the PDE level.

3.1. Basic time-stepping algorithm. Based on this new formulation, our multiphysics time-stepping algorithm reads as follows:

Splitting Algorithm (SA):

(i) Set

$$\begin{aligned} \mathbf{u}^0 &= \mathbf{u}_0, & p^0 &= p_0, & q^0 &= q_0 := \operatorname{div} \mathbf{u}_0, \\ \eta^0 &= c_0 p^0 + \alpha q^0, & \xi^0 &= \alpha p^0 - \lambda q^0. \end{aligned}$$

(ii) For $n = 0, 1, 2, \dots$, complete the following three steps:

Step 1: Solve for $(\mathbf{u}^{n+1}, \xi^{n+1})$ such that

$$(3.1) \quad -\mu \operatorname{div} \varepsilon(\mathbf{u}^{n+1}) + \nabla \xi^{n+1} = \mathbf{f}, \quad \text{in } \Omega_T,$$

$$(3.2) \quad \kappa_3 \xi^{n+1} + \operatorname{div} \mathbf{u}^{n+1} = \kappa_1 \eta^{n+\theta} \quad \text{in } \Omega_T,$$

$$(3.3) \quad \tilde{\sigma}(\mathbf{u}^{n+1}, \xi^{n+1}) \mathbf{n} = \mathbf{f}_1 \quad \text{on } \partial\Omega_T.$$

Here $\theta = 0$ or 1 .

Step 2: Solve for η^{n+1} such that

$$(3.4) \quad d_t \eta^{n+1} - \frac{1}{\mu_f} \operatorname{div} [K(\nabla(\kappa_2 \eta^{n+1} + \kappa_1 \xi^{n+1}) - \rho_f \mathbf{g})] = \phi, \quad \text{in } \Omega_T,$$

$$(3.5) \quad \frac{1}{\mu_f} K[\nabla(\kappa_2 \eta^{n+1} + \kappa_1 \xi^{n+1}) - \rho_f \mathbf{g}] \cdot \mathbf{n} = \phi_1 \quad \text{on } \partial\Omega_T.$$

Step 3: Update p^{n+1} and q^{n+1} by

$$(3.6) \quad p^{n+1} = \kappa_1 \xi^{n+1} + \kappa_2 \eta^{n+\theta}, \quad q^{n+1} = \kappa_1 \eta^{n+1} - \kappa_3 \xi^{n+1}.$$

Where $d_t \eta^{n+1} := (\eta^{n+1} - \eta^n) / \Delta t$, Δt denotes the time step size of a uniform partition of the time interval $[0, T]$, and

$$(3.7) \quad \tilde{\sigma}(\mathbf{u}^{n+1}, \xi^{n+1}) := \mu \varepsilon(\mathbf{u}^{n+1}) - \xi^{n+1} I.$$

We note that (3.4) is the implicit Euler scheme, which is chosen just for the ease of presentation, it can be replaced by other time-stepping schemes. (3.5) provides a flux boundary condition for η^{n+1} .

REMARK 3.1. *When $\theta = 0$, Step 1 and Step 2 are decoupled, hence these two sub-problems can be solved independently. On the other hand, when $\theta = 1$, two sub-problems are coupled, hence, they must be solved together.*

3.2. Fully discrete finite element methods. In this section, we consider the space-time discretization which combines the above splitting algorithm with appropriately chosen spatial discretization methods. To the end, we introduce some notation. Assume $\Omega \in \mathbb{R}^d (d = 2, 3)$ is a polygonal domain. Let \mathcal{T}_h be a quasi-uniform triangulation or rectangular partition of Ω with mesh size h , and $\bar{\Omega} = \bigcup_{K \in \mathcal{T}_h} \bar{K}$. Also, let

(\mathbf{X}_h, M_h) be a stable mixed finite element pair, that is, $\mathbf{X}_h \subset \mathbf{H}^1(\Omega)$ and $M_h \subset L^2(\Omega)$ satisfy the inf-sup condition

$$(3.8) \quad \sup_{v_h \in \mathbf{X}_h} \frac{(\operatorname{div} v_h, \varphi_h)}{\|\nabla v_h\|_{L^2(\Omega)}} \geq \beta_0 \|\varphi_h\|_{L^2(\Omega)} \quad \forall \varphi_h \in M_{0h} := M_h \cap L_0^2(\Omega), \quad \beta_0 > 0.$$

A number of stable mixed finite element spaces (\mathbf{X}_h, M_h) have been known in the literature [5]. A well-known example is the following so-called Taylor-Hood element (cf. [1, 5]):

$$\begin{aligned} \mathbf{X}_h &= \{ \mathbf{v}_h \in \mathbf{C}^0(\bar{\Omega}); \mathbf{v}_h|_K \in \mathbf{P}_2(K) \quad \forall K \in \mathcal{T}_h \}, \\ M_h &= \{ \varphi_h \in C^0(\bar{\Omega}); \varphi_h|_K \in P_1(K) \quad \forall K \in \mathcal{T}_h \}. \end{aligned}$$

In the next subsection, we shall only present the analysis for the Taylor-Hood element, but remark that the analysis can be extended to other stable mixed elements. However, piecewise constant space M_h is not recommended because that would result in no rate of convergence for the approximation of the pressure p (see Section 3.4).

Finite element approximation space W_h for η variable can be chosen independently, any piecewise polynomial space is acceptable provided that $W_h \supset M_h$. Especially, $W_h \subset L^2(\Omega)$ can be chosen as a fully discontinuous piecewise polynomial space, although it is more convenient to choose W_h to be a continuous (resp. discontinuous) space if M_h is a continuous (resp. discontinuous) space. The most convenient choice is $W_h = M_h$, which will be adopted in the remainder of this paper.

Recall that \mathbf{RM} denotes the space of the infinitesimal rigid motions (see Section 2), evidently, $\mathbf{RM} \subset \mathbf{X}_h$. We now introduce the L^2 -projection \mathcal{P}_R from $\mathbf{L}^2(\Omega)$ to \mathbf{RM} . For each $\mathbf{v} \in \mathbf{L}^2(\Omega)$, $\mathcal{P}_R \mathbf{v}_h \in \mathbf{RM}$ is defined by

$$(\mathcal{P}_R \mathbf{v}_h, \mathbf{r}) = (\mathbf{v}_h, \mathbf{r}) \quad \forall \mathbf{r} \in \mathbf{RM}.$$

Moreover, we define

$$(3.9) \quad \mathbf{V}_h := (I - \mathcal{P}_R) \mathbf{X}_h = \{ \mathbf{v}_h \in \mathbf{X}_h; (\mathbf{v}_h, \mathbf{r}) = 0 \quad \forall \mathbf{r} \in \mathbf{RM} \}.$$

It is easy to check that $\mathbf{X}_h = \mathbf{V}_h \oplus \mathbf{RM}$. It was proved in [11] that there holds the following alternative version of the above inf-sup condition:

$$(3.10) \quad \sup_{\mathbf{v}_h \in \mathbf{V}_h} \frac{(\operatorname{div} \mathbf{v}_h, \varphi_h)}{\|\nabla \mathbf{v}_h\|_{L^2(\Omega)}} \geq \beta_1 \|\varphi_h\|_{L^2(\Omega)} \quad \forall \varphi_h \in M_{0h}, \quad \beta_1 > 0.$$

Finite Element Algorithm (FEA):

- (i) Compute $\mathbf{u}_h^0 \in \mathbf{V}_h$ and $q_h^0 \in W_h$ by

$$\begin{aligned} \mathbf{u}_h^0 &= \mathcal{R}_h \mathbf{u}_0, & p_h^0 &= \mathcal{Q}_h p_0, & q_h^0 &= \mathcal{Q}_h q_0 \quad (q_0 = \operatorname{div} \mathbf{u}_0), \\ \eta_h^0 &= c_0 p_h^0 + \alpha q_h^0, & \xi_h^0 &= \alpha p_h^0 - \lambda q_h^0. \end{aligned}$$

- (ii) For $n = 0, 1, 2, \dots$, do the following three steps.

Step 1: Solve for $(\mathbf{u}_h^{n+1}, \xi_h^{n+1}) \in \mathbf{V}_h \times W_h$ such that

$$(3.11) \quad \mu(\varepsilon(\mathbf{u}_h^{n+1}), \varepsilon(\mathbf{v}_h)) - (\xi_h^{n+1}, \operatorname{div} \mathbf{v}_h) = (\mathbf{f}, \mathbf{v}_h) + \langle \mathbf{f}_1, \mathbf{v}_h \rangle \quad \forall \mathbf{v}_h \in \mathbf{V}_h,$$

$$(3.12) \quad \kappa_3(\xi_h^{n+1}, \varphi_h) + (\operatorname{div} \mathbf{u}_h^{n+1}, \varphi_h) = \kappa_1(\eta_h^{n+\theta}, \varphi_h) \quad \forall \varphi_h \in M_h.$$

Step 2: Solve for $\eta_h^{n+1} \in W_h$ such that

$$(3.13) \quad \begin{aligned} (d_t \eta_h^{n+1}, \psi_h) + \frac{1}{\mu_f} (K(\nabla(\kappa_1 \xi_h^{n+1} + \kappa_2 \eta_h^{n+1}) - \rho_f \mathbf{g}), \nabla \psi_h) \\ = (\phi, \psi_h) + \langle \phi_1, \psi_h \rangle. \end{aligned}$$

Step 3: Update p_h^{n+1} and q_h^{n+1} by

$$(3.14) \quad p_h^{n+1} = \kappa_1 \xi_h^{n+1} + \kappa_2 \eta_h^{n+\theta}, \quad q_h^{n+1} = \kappa_1 \eta_h^{n+1} - \kappa_3 \xi_h^{n+1}.$$

REMARK 3.2. *At each time step, problem (3.11)–(3.12) is a generalized Stokes problem with a mixed boundary condition for (\mathbf{u}, p) . The well-posedness of the generalized Stokes problem follows easily with the help of the inf-sup condition.*

3.3. Stability analysis of fully discrete finite element methods. The primary goal of this subsection is to derive a discrete energy law which mimics the PDE energy law (2.28). It turns out that such a discrete energy law only holds if h and Δt satisfy the mesh constraint $\Delta t = O(h^2)$ when $\theta = 0$ but for all $h, \Delta t > 0$ when $\theta = 1$.

Before discussing the stability of (FEA), We first show that the numerical solution satisfies all side constraints which are fulfilled by the PDE solution.

LEMMA 3.1. *Let $\{(\mathbf{u}_h^n, \xi_h^n, \eta_h^n)\}_{n \geq 0}$ be defined by the (FEA), then there hold*

$$(3.15) \quad (\eta_h^n, 1) = C_\eta(t_n) \quad \text{for } n = 0, 1, 2, \dots,$$

$$(3.16) \quad (\xi_h^n, 1) = C_\xi(t_{n-1+\theta}) \quad \text{for } n = 1 - \theta, 1, 2, \dots,$$

$$(3.17) \quad \langle \mathbf{u}_h^n \cdot \mathbf{n}, 1 \rangle = C_{\mathbf{u}}(t_{n-1+\theta}) \quad \text{for } n = 1 - \theta, 1, 2, \dots$$

Proof. Taking $\psi_h = 1$ in (3.13) yields

$$(d_t \eta_h^{n+1}, 1) = (\phi, 1) + \langle \phi_1, 1 \rangle.$$

Then summing over n from 0 to $\ell (\geq 0)$ we get

$$(\eta_h^{\ell+1}, 1) = (\eta_h^0, 1) + [(\phi, 1) + \langle \phi_1, 1 \rangle] t_{\ell+1} = (\eta_0, 1) + [(\phi, 1) + \langle \phi_1, 1 \rangle] t_{\ell+1} = C_\eta(t_{\ell+1})$$

for $\ell = 0, 1, 2, \dots$. So (3.15) holds.

To prove (3.16), taking $\mathbf{v}_h = \mathbf{x}$ in (3.11) and $\varphi_h = 1$ in (3.12), we get

$$(3.18) \quad \mu(\operatorname{div} \mathbf{u}_h^{n+1}, 1) - d(\xi_h^{n+1}, 1) = (\mathbf{f}, x) + \langle \mathbf{f}_1, x \rangle,$$

$$(3.19) \quad \kappa_3(\xi_h^{n+1}, 1) + (\operatorname{div} \mathbf{u}_h^{n+1}, 1) = \kappa_1 C_\eta(t_{n+\theta}).$$

Substituting (3.19) into (3.18) yields

$$(d + \mu \kappa_3)(\xi_h^{n+1}, 1) = \mu \kappa_1 C_\eta(t_{n+\theta}) - (\mathbf{f}, x) - \langle \mathbf{f}_1, x \rangle.$$

Hence, by the definition of $C_\xi(t)$ we conclude that (3.16) holds for all $n \geq 1 - \theta$.

(3.17) follows from (3.15), (3.16), (3.19), and an application of the Divergence Theorem. The proof is complete. \square

The next lemma establishes an identity which mimics the continuous energy law for the solution of (FEA).

LEMMA 3.2. *Let $\{(\mathbf{u}_h^n, \xi_h^n, \eta_h^n)\}_{n \geq 0}$ be defined by (FEA), then there holds the following identity:*

$$(3.20) \quad J_{h,\theta}^\ell + S_{h,\theta}^\ell = J_{h,\theta}^0 \quad \text{for } \ell \geq 1, \theta = 0, 1,$$

where

$$J_{h,\theta}^\ell := \frac{1}{2} \left[\mu \|\varepsilon(\mathbf{u}_h^{\ell+1})\|_{L^2(\Omega)}^2 + \kappa_2 \|\eta_h^{\ell+\theta}\|_{L^2(\Omega)}^2 + \kappa_3 \|\xi_h^{\ell+1}\|_{L^2(\Omega)}^2 - 2(\mathbf{f}, \mathbf{u}_h^{\ell+1}) - 2\langle \mathbf{f}_1, \mathbf{u}_h^{\ell+1} \rangle \right],$$

$$\begin{aligned} S_{h,\theta}^\ell := \Delta t \sum_{n=1}^{\ell} \left[\frac{\mu \Delta t}{2} \|d_t \varepsilon(\mathbf{u}_h^{n+1})\|_{L^2(\Omega)}^2 + \frac{K}{\mu_f} (\nabla p_h^{n+1} - \rho_f \mathbf{g}, \nabla p_h^{n+1}) \right. \\ \left. + \frac{\kappa_2 \Delta t}{2} \|d_t \eta_h^{n+\theta}\|_{L^2(\Omega)}^2 + \frac{\kappa_3 \Delta t}{2} \|d_t \xi_h^{n+1}\|_{L^2(\Omega)}^2 - (\phi, p_h^{n+1}) - \langle \phi_1, p_h^{n+1} \rangle \right. \\ \left. - (1-\theta) \frac{\kappa_1 K \Delta t}{\mu_f} (d_t \nabla \xi_h^{n+1}, \nabla p_h^{n+1}) \right]. \end{aligned}$$

$$p_h^{n+1} := \kappa_1 \xi_h^{n+1} + \kappa_2 \eta_h^{n+\theta}.$$

Proof. Since the proof for the case $\theta = 1$ is exactly same as that of the PDE energy law, so we omit it and leave it to the interested reader to explore. Here we only consider the case $\theta = 0$. Based on (3.12), we can define η_h^{-1} by

$$(3.21) \quad \kappa_1 (\eta_h^{-1}, \varphi_h) = \kappa_3 (\xi_h^0, \varphi_h) + (\operatorname{div} \mathbf{u}_h^0, \varphi_h)$$

Setting $\mathbf{v}_h = d_t \mathbf{u}_h^{n+1}$ in (3.11), $\varphi_h = \xi_h^{n+1}$ in (3.12), and $\psi_h = p_h^{n+1}$ in (3.13) after lowering the degree from $n+1$ to n , we get

$$(3.22) \quad \begin{aligned} \frac{\mu}{2} d_t \|\varepsilon(\mathbf{u}_h^{n+1})\|_{L^2(\Omega)}^2 + \frac{\mu}{2} \Delta t \|d_t \varepsilon(\mathbf{u}_h^{n+1})\|_{L^2(\Omega)}^2 \\ = d_t (\mathbf{f}, \mathbf{u}_h^{n+1}) + d_t \langle \mathbf{f}_1, \mathbf{u}_h^{n+1} \rangle + (\xi_h^{n+1}, \operatorname{div} d_t \mathbf{u}_h^{n+1}), \end{aligned}$$

$$(3.23) \quad \kappa_3 (d_t \xi_h^{n+1}, \xi_h^{n+1}) + (\operatorname{div} d_t \mathbf{u}_h^{n+1}, \xi_h^{n+1}) = \kappa_1 (d_t \eta_h^n, \xi_h^{n+1}),$$

$$(3.24) \quad \begin{aligned} (d_t \eta_h^n, p_h^{n+1}) + \frac{1}{\mu_f} (K (\nabla (\kappa_1 \xi_h^n + \kappa_2 \eta_h^n) - \rho_f \mathbf{g}), \nabla p_h^{n+1}) \\ = (\phi, p_h^{n+1}) + \langle \phi_1, p_h^{n+1} \rangle. \end{aligned}$$

The first term on the left-hand side of (3.24) can be rewritten as

$$(3.25) \quad \begin{aligned} (d_t \eta_h^n, p_h^{n+1}) &= (d_t \eta_h^n, \kappa_1 \xi_h^{n+1} + \kappa_2 \eta_h^n) \\ &= \kappa_1 (d_t \eta_h^n, \xi_h^{n+1}) + \frac{\kappa_2 \Delta t}{2} \|d_t \eta_h^n\|_{L^2(\Omega)}^2 + \frac{\kappa_2}{2} d_t \|\eta_h^n\|_{L^2(\Omega)}^2. \end{aligned}$$

Moreover,

$$(3.26) \quad \begin{aligned} \frac{K}{\mu_f} (\nabla (\kappa_1 \xi_h^n + \kappa_2 \eta_h^n) - \rho_f \mathbf{g}, \nabla p_h^{n+1}) \\ = \frac{K}{\mu_f} (\nabla p_h^{n+1} - \rho_f \mathbf{g}, \nabla p_h^{n+1}) - \frac{\kappa_1 K \Delta t}{\mu_f} (d_t \nabla \xi_h^{n+1}, \nabla p_h^{n+1}). \end{aligned}$$

$$(3.27) \quad \kappa_3 (d_t \xi_h^{n+1}, \xi_h^{n+1}) = \frac{\kappa_3}{2} d_t \|\xi_h^{n+1}\|_{L^2(\Omega)}^2 + \frac{\kappa_3 \Delta t}{2} \|d_t \xi_h^{n+1}\|_{L^2(\Omega)}^2.$$

Adding (3.22)–(3.24), using (3.25)–(3.27) and applying the summation operator $\Delta t \sum_{n=1}^{\ell}$ to the both sides of the resulting equation yield the desired equality (3.20). The proof is complete. \square

In the case $\theta = 1$, (3.20) gives the desired solution estimates without any mesh constraint. On the other hand, when $\theta = 0$, since the last term in the expression of $S_{h,\theta}^\ell$ does not have a fixed sign, hence, it needs to be controlled in order to ensure the positivity of $S_{h,\theta}^\ell$.

COROLLARY 3.3. *Let $\{(\mathbf{u}_h^n, \xi_h^n, \eta_h^n)\}_{n \geq 0}$ be defined by (FEA) with $\theta = 0$, then there holds the following inequality:*

$$(3.28) \quad J_{h,0}^\ell + \widehat{S}_{h,0}^\ell \leq J_{h,0}^0 \quad \text{for } \ell \geq 1,$$

provided that $\Delta t = O(h^2)$. Where

$$\begin{aligned} \widehat{S}_{h,0}^\ell := \Delta t \sum_{n=1}^{\ell} & \left[\frac{\mu \Delta t}{4} \|d_t \varepsilon(\mathbf{u}_h^{n+1})\|_{L^2(\Omega)}^2 + \frac{K}{2\mu_f} \|\nabla p_h^{n+1}\|_{L^2(\Omega)}^2 - \frac{K}{\mu_f} (\rho_f \mathbf{g}, \nabla p_h^{n+1}) \right. \\ & \left. + \frac{\kappa_2 \Delta t}{2} \|d_t \eta_h^n\|_{L^2(\Omega)}^2 + \frac{\kappa_3 \Delta t}{2} \|d_t \xi_h^{n+1}\|_{L^2(\Omega)}^2 - (\phi, p_h^{n+1}) - \langle \phi_1, p_h^{n+1} \rangle \right]. \end{aligned}$$

Proof. By Schwarz inequality and inverse inequality (3.31), we get

$$(3.29) \quad \begin{aligned} \frac{\kappa_1 K \Delta t}{\mu_f} (d_t \nabla \xi_h^{n+1}, \nabla p_h^{n+1}) & \leq \frac{\kappa_1^2 K}{2\mu_f} \|\nabla \xi_h^{n+1} - \nabla \xi_h^n\|_{L^2(\Omega)}^2 + \frac{K}{2\mu_f} \|\nabla p_h^{n+1}\|_{L^2(\Omega)}^2 \\ & \leq \frac{c_1^2 \kappa_1^2 K}{2\mu_f h^2} \|\xi_h^{n+1} - \xi_h^n\|_{L(\Omega)_2}^2 + \frac{K}{2\mu_f} \|\nabla p_h^{n+1}\|_{L^2(\Omega)}^2 \end{aligned}$$

To bound the first term on the right-hand side of (3.29), we appeal to the inf-sup condition and get

$$(3.30) \quad \begin{aligned} \|\xi_h^{n+1} - \xi_h^n\|_{L^2} & \leq \frac{1}{\beta_1} \sup_{\mathbf{v}_h \in \mathbf{V}_h} \frac{(\operatorname{div} \mathbf{v}_h, \xi_h^{n+1} - \xi_h^n)}{\|\nabla \mathbf{v}_h\|_{L^2(\Omega)}} \\ & \leq \frac{\mu}{\beta_1} \sup_{\mathbf{v}_h \in \mathbf{V}_h} \frac{(\varepsilon(\mathbf{u}^{n+1} - \mathbf{u}^n), \varepsilon(\mathbf{v}_h))}{\|\nabla \mathbf{v}_h\|_{L^2(\Omega)}} \\ & \leq \frac{\mu}{\beta_1} \Delta t \|d_t \varepsilon(\mathbf{u}_h^{n+1})\|_{L^2}. \end{aligned}$$

Substituting (3.30) into (3.29) and combining it with (3.20) imply (3.28) provided that $\Delta t \leq (\mu_f \beta_1^2) (2\mu K c_1^2 \kappa_1^2)^{-1} h^2$. The proof is complete. \square

3.4. Convergence analysis. The goal of this section is to analyze the fully discrete finite element algorithm (FEA) proposed in the previous subsection. Precisely, we shall derive optimal order error estimates for (FEA) in both $L^\infty(0, T; L^2(\Omega))$ and $L^2(0, T; H^1(\Omega))$ -norm. To the end, we first list some facts, which are well known in the literature [4, 5], about finite element functions.

We first recall the following inverse inequality for polynomial functions [6]:

$$(3.31) \quad \|\nabla \varphi_h\|_{L^2(K)} \leq c_1 h^{-1} \|\varphi_h\|_{L^2(K)} \quad \forall \varphi_h \in P_r(K), K \in T_h.$$

For any $\varphi \in L^2(\Omega)$, we define its L^2 -projection $\mathcal{Q}_h : L^2 \rightarrow W_h$ as

$$(3.32) \quad (\mathcal{Q}_h \varphi, \psi_h) = (\varphi, \psi_h) \quad \psi_h \in W_h.$$

It is well known that the projection operator $\mathcal{Q}_h : L^2 \rightarrow W_h$ satisfies (cf [4]), for any $\varphi \in H^s(\Omega)(s \geq 1)$,

$$(3.33) \quad \|\mathcal{Q}_h\varphi - \varphi\|_{L^2(\Omega)} + h\|\nabla(\mathcal{Q}_h\varphi - \varphi)\|_{L^2(\Omega)} \leq Ch^\ell\|\varphi\|_{H^\ell(\Omega)}, \quad \ell = \min\{2, s\}.$$

We like to point out that when $W_h \notin H^1(\Omega)$, the second term on the left-hand side of (3.33) has to be replaced by the broken H^1 -norm.

Next, for any $\varphi \in H^1(\Omega)$, we define its elliptic projection $\mathcal{S}_h\varphi$ by

$$(3.34) \quad (K\nabla\mathcal{S}_h\varphi, \nabla\varphi_h) = (K\nabla\varphi, \nabla\varphi_h) \quad \varphi_h \in W_h,$$

$$(3.35) \quad (\mathcal{S}_h\varphi, 1) = (\varphi, 1).$$

It is well known that the projection operator $\mathcal{S}_h : H^1(\Omega) \rightarrow W_h$ satisfies (cf [4]), for any $\varphi \in H^s(\Omega)(s > 1)$,

$$(3.36) \quad \|\mathcal{S}_h\varphi - \varphi\|_{L^2(\Omega)} + h\|\nabla(\mathcal{S}_h\varphi - \varphi)\|_{L^2(\Omega)} \leq Ch^\ell\|\varphi\|_{H^\ell(\Omega)}, \quad \ell = \min\{2, s\}.$$

Finally, for any $\mathbf{v} \in \mathbf{H}_\perp^1(\Omega)$, we define its elliptic projection $\mathcal{R}_h\mathbf{v}$ by

$$(3.37) \quad (\varepsilon(\mathcal{R}_h\mathbf{v}), \varepsilon(\mathbf{w}_h)) = (\varepsilon(\mathbf{v}), \varepsilon(\mathbf{w}_h)) \quad \mathbf{w}_h \in \mathbf{V}_h.$$

It is easy to show that the projection $\mathcal{R}_h\mathbf{v}$ satisfies (cf [4]), for any $\mathbf{v} \in \mathbf{H}_\perp^1(\Omega) \cap \mathbf{H}^s(\Omega)(s > 1)$,

$$(3.38) \quad \|\mathcal{R}_h\mathbf{v} - \mathbf{v}\|_{L^2(\Omega)} + h\|\nabla(\mathcal{R}_h\mathbf{v} - \mathbf{v})\|_{L^2(\Omega)} \leq Ch^m\|\mathbf{v}\|_{H^m(\Omega)}, \quad m = \min\{3, s\}.$$

To derive error estimates, we introduce the following error notation

$$\begin{aligned} E_{\mathbf{u}}^n &:= \mathbf{u}(t_n) - \mathbf{u}_h^n, & E_\xi^n &:= \xi(t_n) - \xi_h^n, & E_\eta^n &:= \eta(t_n) - \eta_h^n, \\ E_p^n &:= p(t_n) - p_h^n, & E_q^n &:= q(t_n) - q_h^n. \end{aligned}$$

It is easy to check that

$$(3.39) \quad E_p^n = \kappa_1 E_\xi^n + \kappa_2 E_\eta^n, \quad E_q^n = \kappa_3 E_\xi^n + \kappa_1 E_\eta^n.$$

Also, we denote

$$\begin{aligned} E_{\mathbf{u}}^n &= \mathbf{u}(t_n) - \mathcal{R}_h(\mathbf{u}(t_n)) + \mathcal{R}_h(\mathbf{u}(t_n)) - \mathbf{u}_h^n := \Lambda_{\mathbf{u}}^n + \Theta_{\mathbf{u}}^n, \\ E_\xi^n &= \xi(t_n) - \mathcal{S}_h(\xi(t_n)) + \mathcal{S}_h(\xi(t_n)) - \xi_h^n := \Lambda_\xi^n + \Theta_\xi^n, \\ E_\eta^n &= \eta(t_n) - \mathcal{S}_h(\eta(t_n)) + \mathcal{S}_h(\eta(t_n)) - \eta_h^n := \Lambda_\eta^n + \Theta_\eta^n, \\ E_p^n &= p(t_n) - \mathcal{Q}_h(p(t_n)) + \mathcal{Q}_h(p(t_n)) - p_h^n := \Lambda_p^n + \Theta_p^n. \end{aligned}$$

LEMMA 3.4. *Let $\{(\mathbf{u}_h^n, \xi_h^n, \eta_h^n)\}_{n \geq 0}$ be generated by the (FEA) and $\Lambda_{\mathbf{u}}^n, \Theta_{\mathbf{u}}^n, \Lambda_\xi^n, \Theta_\xi^n, \Lambda_\eta^n, \Theta_\eta^n$*

and Θ_η^n be defined as above. Then there holds the following identity:

$$\begin{aligned}
(3.40) \quad & \mathcal{E}_h^\ell + \Delta t \sum_{n=1}^{\ell} \left[\frac{K}{\mu_f} (\nabla \hat{\Theta}_p^{n+1} - \rho_f \mathbf{g}, \hat{\Theta}_p^{n+1}) \right. \\
& \left. + \frac{\Delta t}{2} \left(\mu \|d_t \varepsilon(\Theta_{\mathbf{u}}^{n+1})\|_{L^2(\Omega)}^2 + \kappa_2 \|d_t \Theta_\eta^{n+\theta}\|_{L^2(\Omega)}^2 + \kappa_3 \|d_t \Theta_\xi^{n+1}\|_{L^2(\Omega)}^2 \right) \right] \\
& = \mathcal{E}_h^0 + \Delta t \sum_{n=1}^{\ell} \left[(\Lambda_\xi^{n+1}, \operatorname{div} d_t \Theta_{\mathbf{u}}^{n+1}) - (\operatorname{div} d_t \Lambda_{\mathbf{u}}^{n+1}, \Theta_\xi^{n+1}) \right] \\
& \quad + (\Delta t)^2 \sum_{n=1}^{\ell} (d_t^2 \eta_h(t_{n+1}), \Theta_\xi^{n+1}) + \Delta t \sum_{n=1}^{\ell} (R_h^{n+1}, \hat{\Theta}_p^{n+1}) \\
& \quad + (1-\theta)(\Delta t)^2 \sum_{n=1}^{\ell} \frac{K\kappa_1}{\mu_f} (d_t \nabla \Theta_\xi^{n+1}, \nabla \hat{\Theta}_p^{n+1}),
\end{aligned}$$

where

$$(3.41) \quad \hat{\Theta}_p^{n+1} := \kappa_1 \nabla \Theta_\xi^{n+1} + \kappa_2 \nabla \Theta_\eta^{n+\theta}$$

$$(3.42) \quad \mathcal{E}_h^\ell := \frac{1}{2} \left[\mu \|\varepsilon(\Theta_{\mathbf{u}}^{\ell+1})\|_{L^2(\Omega)}^2 + \kappa_2 \|\Theta_\eta^{\ell+\theta}\|_{L^2(\Omega)}^2 + \kappa_3 \|\Theta_\xi^{\ell+1}\|_{L^2(\Omega)}^2 \right],$$

$$(3.43) \quad R_h^{n+1} := -\frac{1}{\Delta t} \int_{t_n}^{t_{n+1}} (s - t_n) \eta_{tt}(s) ds.$$

Proof. Subtracting (3.11) from (2.21), (3.12) from (2.22), (3.13) from (2.23), respectively, we get the following error equations:

$$(3.44) \quad \mu(\varepsilon(\mathbf{E}_{\mathbf{u}}^{n+1}), \varepsilon(\mathbf{v}_h)) - (E_\xi^{n+1}, \operatorname{div} \mathbf{v}_h) = 0 \quad \forall \mathbf{v}_h \in V_h,$$

$$(3.45) \quad \kappa_3(E_\xi^{n+1}, \varphi_h) + (\operatorname{div} \mathbf{E}_{\mathbf{u}}^{n+1}, \varphi_h) \\ = \kappa_1(E_\eta^{n+\theta}, \varphi_h) + \Delta t (d_t \eta(t_{n+1}), \varphi_h) \quad \forall \varphi_h \in M_h,$$

$$(3.46) \quad (d_t E_\eta^{n+1}, \psi_h) + \frac{K}{\mu_f} (\nabla(\kappa_1 E_\xi^{n+1} + \kappa_2 E_\eta^{n+1}) - \rho_f \mathbf{g}, \nabla \psi_h) \\ = (R_h^{n+1}, \psi_h) \quad \forall \psi_h \in W_h,$$

$$(3.47) \quad E_{\mathbf{u}}^0 = 0, \quad E_\xi^0 = 0, \quad E_\eta^{-1} = 0.$$

Using the definition of the projection operators $\mathcal{Q}_h, \mathcal{S}_h, \mathcal{R}_h$, we have

$$(3.48) \quad \mu(\varepsilon(\Theta_{\mathbf{u}}^{n+1}), \varepsilon(\mathbf{v}_h)) - (\Theta_\xi^{n+1}, \operatorname{div} \mathbf{v}_h) = (\Lambda_\xi^{n+1}, \operatorname{div} \mathbf{v}_h), \quad \forall \mathbf{v}_h \in V_h,$$

$$(3.49) \quad \kappa_3(\Theta_\xi^{n+1}, \varphi_h) + (\operatorname{div} \Theta_{\mathbf{u}}^{n+1}, \varphi_h) = \kappa_1(\Theta_\eta^{n+\theta}, \varphi_h) \\ - (\operatorname{div} \Lambda_{\mathbf{u}}^{n+1}, \varphi_h) + \Delta t (d_t \eta(t_{n+1}), \varphi_h) \quad \forall \varphi_h \in M_h,$$

$$(3.50) \quad (d_t \Theta_\eta^{n+1}, \psi_h) + \frac{K}{\mu_f} (\nabla(\kappa_1 \Theta_\xi^{n+1} + \kappa_2 \Theta_\eta^{n+1}) - \rho_f \mathbf{g}, \nabla \psi_h) \\ = (R_h^{n+1}, \psi_h) \quad \forall \psi_h \in W_h,$$

$$(3.51) \quad E_{\mathbf{u}}^0 = 0, \quad E_\xi^0 = 0, \quad E_\eta^{-1} = 0.$$

(3.40) follows from setting $\mathbf{v}_h = d_t \Theta_{\mathbf{u}}^{n+1}$ in (3.48), $\varphi_h = \Theta_\xi^{n+1}$ (after applying the difference operator d_t to the equation (3.49)), $\psi_h = \hat{\Theta}_p^{n+1} = \kappa_1 \Theta_\xi^{n+1} + \kappa_2 \Theta_\eta^{n+\theta}$ in

(3.50), adding the resulting equations, and applying the summation operator $\Delta t \sum_{n=1}^{\ell}$ to both sides. \square

THEOREM 3.5. *Let $\{(u_h^n, \xi_h^n, \eta_h^n)\}_{n \geq 0}$ be defined by (FEA), then there holds the error estimate for $\ell \leq N$*

$$(3.52) \quad \max_{0 \leq n \leq \ell} \left[\sqrt{\mu} \|\varepsilon(\Theta_{\mathbf{u}}^{n+1})\|_{L^2(\Omega)} + \sqrt{\kappa_2} \|\Theta_{\eta}^{n+\theta}\|_{L^2(\Omega)} + \sqrt{\kappa_3} \|\Theta_{\xi}^{n+1}\|_{L^2(\Omega)} \right] \\ + \left[\Delta t \sum_{n=0}^{\ell} \frac{K}{\mu_f} \|\hat{\Theta}_p^{n+1}\|_{L^2}^2 \right]^{\frac{1}{2}} \leq C_1(T) \Delta t + C_2(T) h^2,$$

provided that $\Delta t = O(h^2)$ when $\theta = 0$ and $\Delta t > 0$ when $\theta = 1$. Where

$$(3.53) \quad C_1(T) = C \|q_t\|_{L^2((0,T);L^2(\Omega))}^2 + C \|(q)_{tt}\|_{L^2((0,T);H^{-1}(\Omega))},$$

$$(3.54) \quad C_2(T) = C \|\xi\|_{L^\infty((0,T);H^2(\Omega))} + C \|\xi_t\|_{L^2((0,T);H^2(\Omega))} \\ + C \|\operatorname{div}(\mathbf{u})_t\|_{L^2((0,T);H^2(\Omega))}.$$

Proof. To derive the above inequality, we need to bound each term on the right-hand side of (3.40). Using the fact $\Theta_{\mathbf{u}}^0 = \mathbf{0}$, $\Theta_{\xi}^0 = 0$ and $\Theta_{\eta}^{-1} = 0$, we have

$$(3.55) \quad \mathcal{E}_h^\ell + \Delta t \sum_{n=1}^{\ell} \left[\frac{K}{\mu_f} (\nabla \hat{\Theta}_p^{n+1} - \rho_f \mathbf{g}, \nabla \hat{\Theta}_p^{n+1}) \right. \\ \left. + \frac{\Delta t}{2} \left(\mu \|d_t \varepsilon(\Theta_{\mathbf{u}}^{n+1})\|_{L^2(\Omega)}^2 + \kappa_2 \|d_t \Theta_{\eta}^{n+\theta}\|_{L^2(\Omega)}^2 + \kappa_3 \|d_t \Theta_{\xi}^{n+1}\|_{L^2(\Omega)}^2 \right) \right] \\ = (\Delta t)^2 \sum_{n=1}^{\ell} (d_t^2 \eta(t_{n+1}), \Theta_{\xi}^{n+1}) + \Delta t \sum_{n=1}^{\ell} (R_h^{n+1}, \hat{\Theta}_p^{n+1}) + \frac{\mu}{2} \|\varepsilon(\Theta_{\mathbf{u}}^1)\|_{L^2(\Omega)}^2 \\ + \Delta t \sum_{n=1}^{\ell} \left[(\Lambda_{\xi}^{n+1}, \operatorname{div} d_t \Theta_{\mathbf{u}}^{n+1}) - (\operatorname{div} d_t \Lambda_{\mathbf{u}}^{n+1}, \Theta_{\xi}^{n+1}) \right] \\ + (1 - \theta) (\Delta t)^2 \sum_{n=1}^{\ell} \frac{K \kappa_1}{\mu_f} (d_t \nabla \Theta_{\xi}^{n+1}, \nabla \hat{\Theta}_p^{n+1}),$$

We now estimate each term on the right-hand side of (3.55). To bound the first term on the right-hand side of (3.55), we first use the summation by parts formula and $d_t \eta_h(t_0) = 0$ to get

$$(3.56) \quad \sum_{n=0}^{\ell} (d_t^2 \eta(t_{n+1}), \Theta_{\xi}^{n+1}) = \frac{1}{\Delta t} (d_t \eta(t_{l+1}), \Theta_{\xi}^{l+1}) - \sum_{n=1}^{\ell} (d_t \eta(t_n), d_t \Theta_{\xi}^{n+1}).$$

Now, we bound each term on the right-hand side of (3.56) as follows:

$$\begin{aligned}
(3.57) \quad & \frac{1}{\Delta t} (d_t \eta(t_{\ell+1}), \Theta_\xi^{\ell+1}) \leq \frac{1}{\Delta t} \|d_t \eta(t_{\ell+1})\|_{L^2(\Omega)} \|\Theta_\xi^{\ell+1}\|_{L^2(\Omega)} \\
& \leq \frac{1}{\Delta t} \|\eta_t\|_{L^2((t_\ell, t_{\ell+1}); L^2(\Omega))} \cdot \frac{1}{\beta_1} \sup_{\mathbf{v}_h \in \mathbf{V}_h} \frac{\mu(\varepsilon(\Theta_{\mathbf{u}}^{\ell+1}), \varepsilon(\mathbf{v}_h)) - (\Lambda_\xi^{\ell+1}, \operatorname{div} \mathbf{v}_h)}{\|\nabla \mathbf{v}_h\|_{L^2(\Omega)}} \\
& \leq \frac{C\mu}{\beta_1 \Delta t} \|\eta_t\|_{L^2((t_\ell, t_{\ell+1}); L^2(\Omega))} \left[\|\varepsilon(\Theta_{\mathbf{u}}^{\ell+1})\|_{L^2(\Omega)} + \frac{1}{\mu} \|\Lambda_\xi^{\ell+1}\|_{L^2(\Omega)} \right] \\
& \leq \frac{\mu}{4(\Delta t)^2} \|\varepsilon(\Theta_{\mathbf{u}}^{\ell+1})\|_{L^2(\Omega)}^2 + \frac{C\mu}{\beta_1^2} \|\eta_t\|_{L^2((t_\ell, t_{\ell+1}); L^2(\Omega))}^2 + \frac{C}{\beta_1^2} \|\Lambda_\xi^{\ell+1}\|_{L^2(\Omega)}^2, \\
(3.58) \quad & \sum_{n=1}^{\ell} (d_t \eta(t_n), d_t \Theta_\xi^{n+1}) \leq \sum_{n=1}^{\ell} \|d_t \eta(t_n)\|_{L^2(\Omega)} \|d_t \Theta_\xi^{n+1}\|_{L^2(\Omega)} \\
& \leq \sum_{n=1}^{\ell} \|d_t \eta(t_n)\|_{L^2(\Omega)} \cdot \frac{1}{\beta_1} \sup_{\mathbf{v}_h \in \mathbf{V}_h} \frac{\mu(d_t \varepsilon(\Theta_{\mathbf{u}}^{n+1}), \varepsilon(\mathbf{v}_h)) - (d_t \Lambda_\xi^{n+1}, \operatorname{div} \mathbf{v}_h)}{\|\nabla \mathbf{v}_h\|_{L^2(\Omega)}} \\
& \leq \frac{C\mu}{\beta_1} \sum_{n=1}^{\ell} \|d_t \eta(t_n)\|_{L^2(\Omega)} \left[\|d_t \varepsilon(\Theta_{\mathbf{u}}^{n+1})\|_{L^2(\Omega)} + \frac{1}{\mu} \|d_t \Lambda_\xi^{n+1}\|_{L^2(\Omega)} \right] \\
& \leq \sum_{n=1}^{\ell} \left[\frac{\mu}{4} \|d_t \varepsilon(\Theta_{\mathbf{u}}^{n+1})\|_{L^2(\Omega)}^2 + \frac{C}{\beta_1^2} \|d_t \Lambda_\xi^{n+1}\|_{L^2(\Omega)}^2 \right] + \frac{C\mu}{\beta_1^2} \|\eta_t\|_{L^2((0, T); L^2(\Omega))}^2.
\end{aligned}$$

The second term on the right-hand side of (3.55) can be bounded as

$$\begin{aligned}
(3.59) \quad & |(R_h^{n+1}, \hat{\Theta}_p^{n+1})| \leq \|R_h^{n+1}\|_{H^{-1}(\Omega)} \|\nabla \hat{\Theta}_p^{n+1}\|_{L^2(\Omega)} \\
& \leq \frac{K}{4\mu_f} \|\nabla \hat{\Theta}_p^{n+1}\|_{L^2(\Omega)}^2 + \frac{\mu_f}{K} \|R_h^{n+1}\|_{H^{-1}(\Omega)}^2 \\
& \leq \frac{K}{4\mu_f} \|\nabla \hat{\Theta}_p^{n+1}\|_{L^2(\Omega)}^2 + \frac{\mu_f \Delta t}{3K} \|\eta_{tt}\|_{L^2((t_n, t_{n+1}); H^{-1}(\Omega))}^2,
\end{aligned}$$

where we have used the fact that

$$\|R_h^{n+1}\|_{H^{-1}(\Omega)}^2 \leq \frac{\Delta t}{3} \int_{t_n}^{t_{n+1}} \|\eta_{tt}\|_{H^{-1}(\Omega)}^2 dt.$$

The fourth term on the right-hand side of (3.55) can be bounded by

$$\begin{aligned}
(3.60) \quad & \Delta t \sum_{n=1}^{\ell} \left[(\Lambda_\xi^{n+1}, \operatorname{div} d_t \Theta_{\mathbf{u}}^{n+1}) - (\operatorname{div} d_t \Lambda_{\mathbf{u}}^{n+1}, \Theta_\xi^{n+1}) \right] \\
& = (\Lambda_\xi^{\ell+1}, \operatorname{div} \Theta_{\mathbf{u}}^{\ell+1}) - \Delta t \sum_{n=1}^{\ell} \left[(d_t \Lambda_\xi^{n+1}, \operatorname{div} \Theta_{\mathbf{u}}^n) + (\operatorname{div} d_t \Lambda_{\mathbf{u}}^{n+1}, \Theta_\xi^{n+1}) \right] \\
& \leq \frac{1}{2} \|\Lambda_\xi^{\ell+1}\|_{L^2(\Omega)}^2 + \frac{1}{2} \|\operatorname{div} \Theta_{\mathbf{u}}^{\ell+1}\|_{L^2(\Omega)}^2 + \frac{1}{2} \Delta t \sum_{n=1}^{\ell} \left[\|d_t \Lambda_\xi^{n+1}\|_{L^2(\Omega)}^2 \right. \\
& \quad \left. + C \|\varepsilon(\Theta_{\mathbf{u}}^{n+1})\|_{L^2(\Omega)}^2 + \|\operatorname{div} d_t \Lambda_{\mathbf{u}}^{n+1}\|_{L^2(\Omega)}^2 + \|\Theta_\xi^{n+1}\|_{L^2(\Omega)}^2 \right],
\end{aligned}$$

here we have used Korn's inequality

$$\|\operatorname{div} \Theta_{\mathbf{u}}^{n+1}\|_{L^2(\Omega)} \leq C \|\varepsilon(\Theta_{\mathbf{u}}^{n+1})\|_{L^2(\Omega)}.$$

When $\theta = 0$ we also need to bound the last term on the right-hand side of (3.55), which is carried out below.

$$\begin{aligned}
 (3.61) \quad & \sum_{n=1}^{\ell} (d_t \nabla \Theta_{\xi}^{n+1}, \nabla \hat{\Theta}_p^{n+1}) \leq \sum_{n=1}^{\ell} \|d_t \Theta_{\xi}^{n+1}\|_{L^2(\Omega)} \|\nabla \hat{\Theta}_p^{n+1}\|_{L^2(\Omega)} \\
 & \leq \sum_{n=1}^{\ell} \sup_{\mathbf{v}_h \in \mathbf{V}_h} \frac{\mu(d_t \varepsilon(\Theta_{\mathbf{u}}^{n+1}), \varepsilon(\mathbf{v}_h)) - (d_t \Lambda_{\xi}^{n+1}, \operatorname{div} \mathbf{v}_h)}{\|\nabla \mathbf{v}_h\|_{L^2(\Omega)}} \|\nabla \hat{\Theta}_p^{n+1}\|_{L^2(\Omega)} \\
 & \leq \sum_{n=1}^{\ell} \left[\frac{\mu^2 \kappa_1 \Delta t}{h^2 \beta_1^2} \|d_t \varepsilon(\Theta_{\mathbf{u}}^{n+1})\|_{L^2}^2 + \frac{\kappa_1 \Delta t}{h^2 \beta_1^2} \|d_t \Lambda_{\xi}^{n+1}\|_{L^2}^2 + \frac{\kappa_1^{-1}}{4 \Delta t} \|\nabla \hat{\Theta}_p^{n+1}\|_{L^2(\Omega)}^2 \right].
 \end{aligned}$$

Substituting (3.56)–(3.61) into (3.55) and rearranging terms we get

$$\begin{aligned}
 (3.62) \quad & \mu \|\varepsilon(\Theta_{\mathbf{u}}^{\ell+1})\|_{L^2(\Omega)}^2 + \kappa_2 \|\Theta_{\eta}^{\ell+\theta}\|_{L^2(\Omega)}^2 + \kappa_3 \|\Theta_{\xi}^{\ell+1}\|_{L^2(\Omega)}^2 \\
 & + \Delta t \sum_{n=1}^{\ell} \frac{K}{\mu_f} \|\nabla \hat{\Theta}_p^{n+1}\|_{L^2(\Omega)}^2 \\
 & \leq \frac{4\mu_f (\Delta t)^2}{\kappa} \|\eta_t\|_{L^2((0,T);H^{-1})}^2 + \frac{4\mu (\Delta t)^2}{\beta_1^2} \|\eta_t\|_{L^2((0,T);L^2(\Omega))}^2, \\
 & + \|\Lambda_{\xi}^{\ell+1}\|_{L^2(\Omega)}^2 + \Delta t \sum_{n=1}^{\ell} \|d_t \Lambda_{\xi}^{n+1}\|_{L^2(\Omega)}^2 + \Delta t \sum_{n=1}^{\ell} \|\operatorname{div} d_t \Lambda_{\mathbf{u}}^{n+1}\|_{L^2(\Omega)}^2,
 \end{aligned}$$

provide that $\Delta t \leq \mu_f \beta_1^2 (4\mu \kappa_1^2 K)^{-1} h^2$ when $\theta = 0$, but it holds for all $\Delta t > 0$ when $\theta = 1$. Hence, (3.52) follows from using the approximation properties of the projection operators \mathcal{Q}_h , \mathcal{R}_h and \mathcal{S}_h . The proof is complete. \square

We conclude this section by stating the main theorem of the section.

THEOREM 3.6. *The solution of the (FEA) satisfies the following error estimates:*

$$\begin{aligned}
 (3.63) \quad & \max_{0 \leq n \leq N} \left[\sqrt{\mu} \|\nabla(u(t_n) - u_h^n)\|_{L^2(\Omega)} + \sqrt{\kappa_2} \|\eta(t_n) - \eta_h^n\|_{L^2(\Omega)} \right. \\
 & \left. + \sqrt{\kappa_3} \|\xi(t_n) - \xi_h^n\|_{L^2(\Omega)} \right] \leq \hat{C}_1(T) \Delta t + \hat{C}_2(T) h^2.
 \end{aligned}$$

$$(3.64) \quad \left[\Delta t \sum_{n=0}^N \frac{K}{\mu_f} \|\nabla(p(t_n) - p_h^n)\|_{L^2(\Omega)}^2 \right]^{\frac{1}{2}} \leq \hat{C}_1(T) \Delta t + \hat{C}_2(T) h,$$

provided that $\Delta t = O(h^2)$ when $\theta = 0$ and $\Delta t > 0$ when $\theta = 1$. Where

$$\begin{aligned}
 \hat{C}_1(T) & := C_1(T), \\
 \hat{C}_2(T) & := C_2(T) + \|\xi\|_{L^\infty((0,T);H^2(\Omega))} + \|\eta\|_{L^\infty((0,T);H^2(\Omega))} \\
 & \quad + \|\nabla \mathbf{u}\|_{L^\infty((0,T);H^2(\Omega))}.
 \end{aligned}$$

Proof. The above estimates follow immediately from an application of the triangle inequality on

$$\begin{aligned}
 \mathbf{u}(t_n) - \mathbf{u}_h^n & = \Lambda_{\mathbf{u}}^n + \Theta_{\mathbf{u}}^n, & \xi(t_n) - \xi_h^n & = \Lambda_{\xi}^n + \Theta_{\xi}^n, \\
 \eta(t_n) - \eta_h^n & = \Lambda_{\eta}^n + \Theta_{\eta}^n, & p(t_n) - p_h^n & = \hat{\Lambda}_p^n + \hat{\Theta}_p^n.
 \end{aligned}$$

and appealing to (3.33), (3.38) and Theorem 3.5. \square

4. Numerical experiments. In this section we shall present three 2-dimensional numerical experiments to validate theoretical results for the proposed numerical methods, to numerically examine the performances of the approach and methods as well as to compare them with existing methods in the literature on two benchmark problems. One of these two problems was used to demonstrate the “locking phenomenon” in [16]. Our numerical result shows that such a “locking phenomenon” phenomenon does not occur in our numerical methods, it confirms the fact that our approach and methods have a built-in mechanism to prevent the “locking phenomenon”.

Test 1. Let $\Omega = [0, 1] \times [0, 1]$, $\Gamma_1 = \{(1, x_2); 0 \leq x_2 \leq 1\}$, $\Gamma_2 = \{(x_1, 0); 0 \leq x_1 \leq 1\}$, $\Gamma_3 = \{(0, x_2); 0 \leq x_2 \leq 1\}$, $\Gamma_4 = \{(x_1, 1); 0 \leq x_1 \leq 1\}$, and $T = 0.001$. We consider problem (2.23)–(2.26) with following source functions:

$$\begin{aligned} \mathbf{f} &= -(\lambda + \mu)t(1, 1)^T + \alpha \cos(x_1 + x_2)e^t(1, 1)^T, \\ \phi &= \left(c_0 + \frac{2\kappa}{\mu_f}\right) \sin(x_1 + x_2)e^t + \alpha(x_1 + x_2), \end{aligned}$$

and the following boundary and initial conditions:

$$\begin{aligned} p &= \sin(x_1 + x_2)e^t && \text{on } \partial\Omega_T, \\ u_1 &= \frac{1}{2}x_1^2t && \text{on } \Gamma_j \times (0, T), j = 1, 3, \\ u_2 &= \frac{1}{2}x_2^2t && \text{on } \Gamma_j \times (0, T), j = 2, 4, \\ \sigma\mathbf{n} - \alpha p\mathbf{n} &= \mathbf{f}_1, && \text{on } \partial\Omega_T; \\ \mathbf{u}(x, 0) &= \mathbf{0}, \quad p(x, 0) = \sin(x_1 + x_2) && \text{in } \Omega, \end{aligned}$$

where

$$\mathbf{f}_1(x, t) = \mu(x_1n_1, x_2n_2)^T t + \lambda(x_1 + x_2)(n_1, n_2)^T t - \alpha \sin(x_1 + x_2)(n_1, n_2)^T e^t.$$

It is easy to check that the exact solution for this problem is

$$\mathbf{u}(x, t) = \frac{t}{2}(x_1^2, x_2^2)^T, \quad p(x, t) = \sin(x_1 + x_2)e^t.$$

We note that the boundary conditions used above are not pure Neumann conditions, instead, they are mixed Dirichlet-Neumann conditions. As pointed out in Remark 2.1 (c), the approach and methods of this paper also apply to this case, the only change is to replace the test and trial space $\mathbf{H}_\perp^1(\Omega)$ by $\mathbf{H}^1(\Omega)$ with some appropriately built-in Dirichlet boundary condition in Definition 2.2.

The goal of doing this test problem is to compute the order of the exact errors and to show that the theoretical error bounds proved in the previous section are sharp.

Table 4.1 displays the computed $L^\infty(0, T; L^2(\Omega))$ and $L^2(0, T; H^1(\Omega))$ -norm errors and the convergence rates with respect to h at the terminal time T . In the test, $\Delta t = 10^{-5}$ is used so that the time error is negligible. Evidently, the spatial rates of convergence are consistent with that proved in the convergence theorem.

Figures 4.1 and 4.2 show respectively the surface plot of the computed pressure p at the terminal time T and the color plot of both the computed pressure p and displacement \mathbf{u} with mesh parameters $h = 0.02$ and $\Delta t = 10^{-5}$. They coincide with the exact solution on the same space-time resolution.

	$L^\infty(L^2)$ error	$L^\infty(L^2)$ order	$L^2(H^1)$ error	$L^2(H^1)$ order
$h = 0.16$	2.0789e-3		5.5045e-2	
$h = 0.08$	5.9674e-4	1.8006	2.9431e-2	0.9032
$h = 0.04$	1.6227e-4	1.8787	1.5332e-2	0.9408
$h = 0.02$	4.0971e-5	1.9857	7.6968e-3	0.9942

TABLE 4.1
Spatial errors and convergence rates of Test 1.

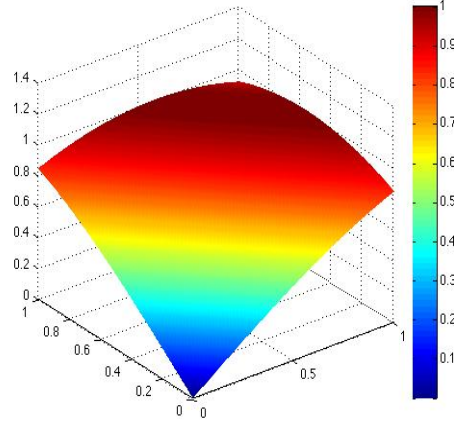


FIG. 4.1. Test 1: Surface plot of the Computed pressure p at the terminal time T .

Test 2. In this test we consider so-called Barry-Mercer's problem, which is a Benchmark test problem for the poroelasticity model (2.23)–(2.26) (cf. [18, 16] and the references therein). Again, $\Omega = [0, 1] \times [0, 1]$ but $T = 1$. Barry-Mercer's problem assumes no source, that is, $\mathbf{f} \equiv 0$ and $\phi \equiv 0$, and takes the following boundary conditions:

$$\begin{aligned}
 p &= 0 && \text{on } \Gamma_j \times (0, T), j = 1, 3, 4, \\
 p &= p_2 && \text{on } \Gamma_j \times (0, T), j = 2, \\
 u_1 &= 0 && \text{on } \Gamma_j \times (0, T), j = 1, 3, \\
 u_2 &= 0 && \text{on } \Gamma_j \times (0, T), j = 2, 4, \\
 \sigma \mathbf{n} - \alpha \mathbf{p} \mathbf{n} &= \mathbf{f}_1 := (0, \alpha p)^T && \text{on } \partial\Omega_T,
 \end{aligned}$$

where

$$p_2(x_1, t) = \begin{cases} \sin t & \text{when } x \in [0.2, 0.8] \times (0, T), \\ 0 & \text{others.} \end{cases}$$

The boundary segments $\Gamma_j, j = 1, 2, 3, 4$, which are defined in **Test 1**, and the above boundary conditions are depicted in Figure 4.3. Also, the initial conditions for Barry-Mercer's problem are $\mathbf{u}(x, 0) \equiv \mathbf{0}$ and $p(x, 0) \equiv 0$. We remark that Barry-Mercer's problem has a unique solution which is given by an infinite series (cf. [16]).

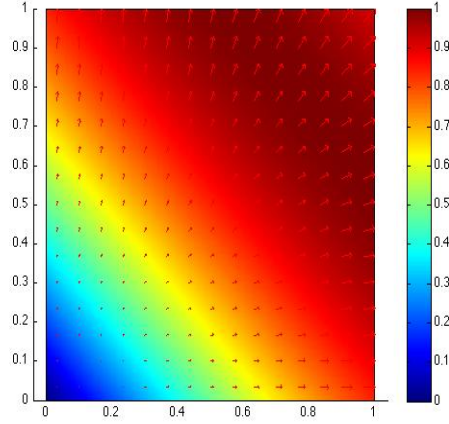


FIG. 4.2. *Test 1: Computed pressure p (color plot) and displacement \mathbf{u} (arrow plot) at T .*

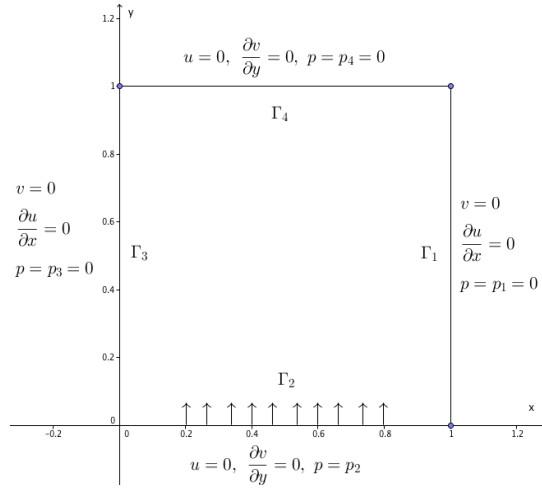
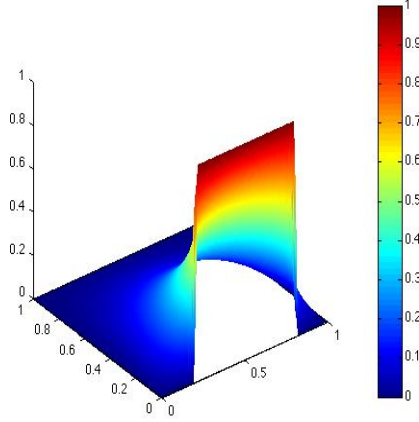
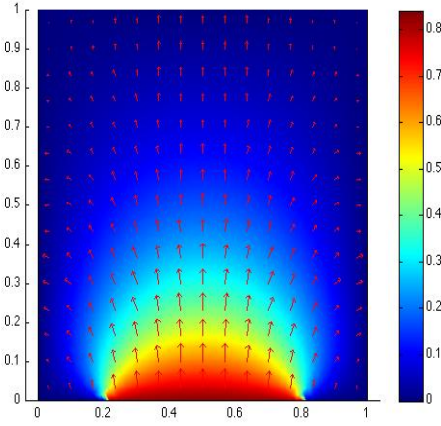


FIG. 4.3. *Test 2: boundary conditions.*

Figures 4.4 and 4.5 display respectively the computed pressure p (surface plot) and the computed displacement \mathbf{u} (arrow plot). We note that the arrows near the boundary match very well with those on the boundary. Our numerical solution approximates the exact solution of Barry-Mercer's problem very well and does not produce any oscillation in computed pressure.

Test 3. This test problem is taken from [16]. Again, we consider problem (2.23)–(2.26) with $\Omega = [0, 1] \times [0, 1]$. Let Γ_j be same as in **Test 1** and $c_0 = 0, E = 10^5, \nu = 0.4, \mu = 35714$ and $T = 0.001$. There is no source, that is, $\mathbf{f} \equiv 0$ and $\phi \equiv 0$. The


 FIG. 4.4. Test 2: Surface plot of the computed pressure p at the terminal time T .

 FIG. 4.5. Test 2: Computed pressure p (color plot) and displacement (arrow plot) at T .

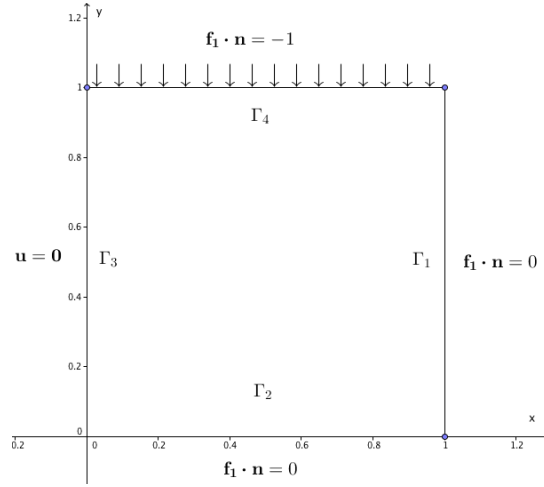
boundary conditions are taken as

$$\begin{aligned} -\frac{\kappa}{\mu_f}(\nabla p - \rho_f \mathbf{g}) \cdot \mathbf{n} &= 0 && \text{on } \partial\Omega_T, \\ \mathbf{u} &= \mathbf{0} && \text{on } \Gamma_3 \times (0, T), \\ \boldsymbol{\sigma} \mathbf{n} - \alpha \mathbf{p} \mathbf{n} &= \mathbf{f}_1 && \text{on } \Gamma_j \times (0, T), \quad j = 1, 2, 4, \end{aligned}$$

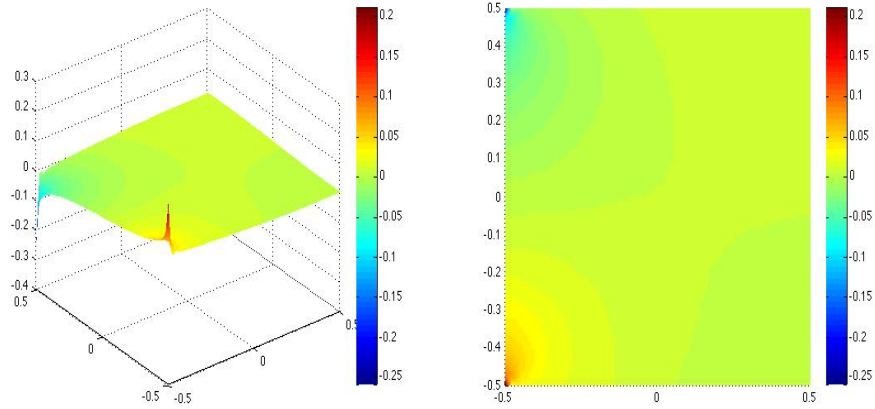
where $\mathbf{f}_1 = (f_1^1, f_1^2)$ and

$$f_1^1 \equiv 0 \quad \text{on } \partial\Omega_T, \quad f_1^2 = \begin{cases} 0 & \text{on } \Gamma_j \times (0, T), \quad j = 1, 2, 3, \\ -1 & \text{on } \Gamma_4 \times (0, T). \end{cases}$$

The computational domain Ω and the above boundary conditions are depicted in Figure 4.6. Also, the zero initial conditions are assigned for both \mathbf{u} and p in this test.

FIG. 4.6. *Test 3: boundary conditions*

Figures 4.7–4.8 display respectively the surface and color plot of the computed pressure, the arrow plot of the displacement vector, and the deformation of the whole Ω . There is no oscillation in the computed pressure and the arrows near the boundary match very well with arrows on the boundary.

FIG. 4.7. *Test 3: Computed pressure p : surface plot (left) and color plot (right).*

We remark that the “locking phenomenon” was observed in the simulation of [16] at $T = 0.001$ for this problem, namely, the computed pressure exhibits some oscillation at $T = 0.001$. The reason for the locking phenomenon was explained as follows: when time step Δt is small, the displacement vector \mathbf{u} is almost divergence free in the short time while the numerical solution does not observe this nearly divergence free property, which results in the locking. However, at later times the displacement vector is no longer divergence free, so no locking exists at later times.

It is clear that our numerical solution does not exhibit the locking phenomenon at $T = 0.001$. This is because our multiphysics reformulation weakly imposes the

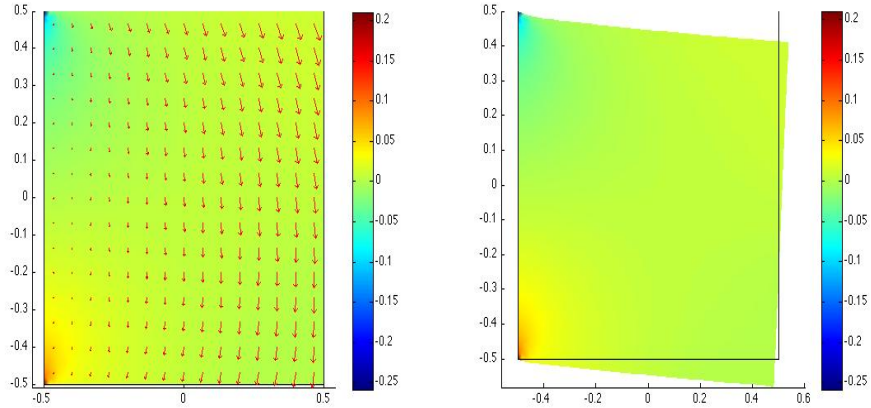


FIG. 4.8. Test 3: Arrow plot of the computed displacement (left) and deformation of Ω (right).

condition $\operatorname{div} \mathbf{u} = q$, hence, \mathbf{u} automatically becomes nearly divergence free when $q \approx 0$ for $0 < t \ll 1$. Moreover, the pressure p is not a primary variable anymore in our reformulation, instead, p becomes a derivative variable and it is computed using the new primary variables ξ and η . Therefore, our numerical methods are insensitive to the regularity of p .

REFERENCES

- [1] J. Bercovier and O. Pironneau, *Error estimates for finite element solution of the Stokes problem in the primitive variables*, Numer. Math., 33, pp. 211–224, (1979).
- [2] M. Biot, *Theory of elasticity and consolidation for a porous anisotropic media*, J. Appl. Phys. 26, pp. 182–185 (1955).
- [3] S. C. Brenner, *A nonconforming mixed multigrid method for the pure displacement problem in planar linear elasticity*, SIAM J. Numer. Anal., 30, pp. 116–135 (1993).
- [4] S. C. Brenner and L. R. Scott, *The Mathematical Theory of Finite Element Methods*, third edition, Springer, 2008.
- [5] F. Brezzi and M. Fortin, *Mixed and Hybrid Finite Element Methods*, Springer, New York, 1992.
- [6] P.G. Ciarlet, *The Finite Element Method for Elliptic Problems*, North-Holland, Amsterdam, 1978.
- [7] O. Coussy, *Poromechanics*, Wiley & Sons, 2004.
- [8] M. Dauge, *Elliptic Boundary Value Problems on Corner Domains*, Lecture Notes in Math., vol. 1341, Springer-Verlag, Berlin, 1988.
- [9] M. Doi and S. F. Edwards, *The Theory of Polymer Dynamics*, Clarendon Press, Oxford, 1986.
- [10] R. Dautray and J. L. Lions, *Mathematical Analysis and Numerical Methods for Science and Technology. Vol. 1*, Springer-Verlag, 1990.
- [11] X. Feng and Y. He, *Fully discrete finite element approximations of a polymer gel model*, SIAM J. Numer. Anal. 48, pp. 2186–2217 (2010).
- [12] D. Gilbarg, N.S. Trudinger, *Elliptic Partial Differential Equations of Second Order*, Second Edition, Springer, New York, 2000.
- [13] V. Girault and P.A. Raviart, *Finite Element Method for Navier-Stokes Equations: theory and algorithms*, Springer-Verlag, Berlin, Heidelberg, New York, 1981.
- [14] I. Hamley, *Introduction to Soft Matter*, John Wiley & Sons, 2007.
- [15] O. A. Ladyženskaja, V. A. Solonnikov and N. N. Uralceva, *Linear and quasilinear equations of parabolic type*, Translations of Mathematical Monographs, Vol. 23, American Mathematical Society, Providence, R.I., 1967.
- [16] P. J. Phillips and M. F. Wheeler, *Overcoming the problem of locking in linear elasticity and poroelasticity: an heuristic approach*. Comput. Geosci. 13, pp. 1–15, (2009).

- [17] P. J. Phillips and M. F. Wheeler, *A coupling of mixed and continuous Galerkin finite element methods for poroelasticity I: the continuous in time case*, Comput. Geosci. 11, pp. 131–144 (2007).
- [18] P. J. Phillips and M. F. Wheeler, *A coupling of mixed and continuous Galerkin finite element methods for poroelasticity II: the discrete in time case*, Comput. Geosci. 11, pp. 145–158 (2007).
- [19] M. A. Murad and A. F. D. Loula, *Improved accuracy in finite element analysis of Biot's consolidation problem*, Comput. Methods in Appl. Mech. and Engr, 95, pp. 359–382 (1992).
- [20] J.E. Roberts and J.M. Thomas, *Mixed and hybrid methods*, in Handbook of Numerical Analysis, Vol. II, North-Holland, New York,, pp. 523–639 (1991).
- [21] L. Schreyer-Bennethum, *Theory of flow and deformation of swelling porous materials at the macroscale*, Computers and Geotechnics, 34, pp. 267-278, 2007.
- [22] R. E. Schowalter, *Diffusion in poro-elastic media*, J. Math. Anal. 251, pp. 310–340 (2000).
- [23] T. Tanaka and D. J. Fillmore, *Kinetics of swelling of gels*, J. Chem. Phys. 70, 1214 (1979).
- [24] K. Terzaghi, *Theoretical Soil Mechanics*, John Wiley & Sons, New York, 1943.
- [25] R. Temam, *Navier-Stokes Equations*, Studies in Mathematics and its Applications, Vol. 2, North-Holland, 1977.
- [26] T. Yamaue and M. Doi, *Swelling dynamics of constrained thin-plate under an external force*, Phys. Rev. E 70, 011401 (2004).